ELECTRODEPOSITION AND CHARACTERIZATION OF NICKEL/TITANIUM CARBIDE NANOCOMPOSITES

A THESIS SUBMITTED TO
THE GRADUATE SCHOOL OF NATURAL AND APPLIED SCIENCES
OF
MIDDLE EAST TECHNICAL UNIVERSITY

BY

NURCAN ACET

IN PARTIAL FULFILLMENT OF THE REQUIREMENTS
FOR
THE DEGREE OF MASTER OF SCIENCE
IN
CHEMICAL ENGINEERING

JUNE 2017

Approval of the thesis:

ELECTRODEPOSITION AND CHARACTERIZATION OF NICKEL/TITANIUM CARBIDE NANOCOMPOSITES

submitted by **NURCAN ACET** partial fulfillment of the requirements for the degree of **Master of Science in Chemical Engineering Department, Middle East Technical University** by,

Prof. Dr. Gülbin Dural Ünver
Dean, Graduate School of **Natural and Applied Sciences** _____

Prof. Dr. Halil Kalıpçılar
Head of Department, **Chemical Engineering** _____

Asst. Prof. Dr. Damla Eroğlu Pala
Supervisor, **Chemical Engineering Dept., METU** _____

Examining Committee Members:

Prof. Dr. Tayfur Öztürk
Metallurgical and Materials Engineering Dept., METU _____

Asst. Prof. Dr. Damla Eroğlu Pala
Chemical Engineering Dept., METU _____

Asst. Prof. Dr. Harun Koku
Chemical Engineering Dept., METU _____

Asst. Prof. Dr. Erhan Bat
Chemical Engineering Dept., METU _____

Asst. Prof. Dr. Burak Ülgüt
Chemistry Dept., Bilkent University _____

Date: 19.06.2017

I hereby declare that all information in this document has been obtained and presented in accordance with academic rules and ethical conduct. I also declare that, as required by these rules and conduct, I have fully cited and referenced all material and results that are not original to this work.

Name, Last Name: Nurcan ACET

Signature:

ABSTRACT

ELECTRODEPOSITION AND CHARACTERIZATION OF NICKEL/TITANIUM CARBIDE NANOCOMPOSITES

Acet, Nurcan
M.Sc., Department of Chemical Engineering
Supervisor: Asst. Prof. Dr. Damla Eroğlu Pala

June 2017, 95 pages

Due to their high hardness, anti-corrosion and anti-wear properties, Nickel/ceramic particle composites have gained significant attention as environmentally-friendly alternatives to chromium and cadmium based coatings typically used in the aerospace industry. Electrodeposition of these Ni/ceramic particle composites has the advantage of lower operating cost and operating temperature than the conventional production methods. Incorporation of ceramic nanoparticles into the Ni matrix has a significant effect on the tribological and mechanical properties of these composites. However, high and uniform particle incorporation into the deposit depends greatly on the dispersion of these nanoparticles in the electrolyte. Therefore, to get superior properties, the agglomeration of the nanoparticles in the electrolyte should be decreased while increasing the nanoparticle incorporation into the deposit. However, a major challenge in this regard is that the dispersants that are used to stabilize the particles in the electrolyte can significantly affect the electrodeposition kinetics.

The aim of this study is to investigate the effect of a cationic dispersant which is polyethyleneimine (PEI) on the electrodeposition of Ni/TiC nanocomposites. The

effect of the dispersant on the particle stability in the electrolyte, on the nanoparticle incorporation rate into the deposit as well as on the electrodeposition kinetics were investigated. Firstly, zeta potential measurements were performed in order to determine the effect of PEI on the particle dispersion in the electrolyte. Secondly, the effect of PEI on the electrodeposition kinetics was investigated using Linear Sweep Voltammetry (LSV) technique and current efficiency measurements. Finally, the amount of TiC in the nanocomposite was analyzed using Scanning Electron Microscopy/Energy Dispersive X-Ray Spectroscopy (SEM/EDS). The optimum PEI bath concentration that increases particle dispersion in the electrolyte and TiC vol.% in the nanocomposite without suppressing the electrodeposition was determined as 125 ppm. In addition, the effect of particle bath concentration on the Ni/TiC electrodeposition was characterized and the optimum TiC concentration was determined as 5 g L^{-1}. Moreover, the effect of current density on the Ni/TiC electrodeposition was investigated and it was seen that TiC incorporation decreases with increasing current density. The effect of rotation speed on TiC incorporation was also characterized and the highest incorporation was achieved at 900 rpm rotation speed. Finally, morphological and mechanical characterization of produced nanocomposites were done and compared to pure Ni coating. Uniform distribution of TiC particles in the metal matrix was observed with the addition of 125 ppm PEI into the electrolyte. Furthermore, the hardness of Ni/TiC nanocomposites was higher than pure Ni coating.

Keywords: Electrodeposition, Metal/ceramic particle nanocomposite, Ni/TiC nanocomposite, Ni/TiC co-deposition, dispersant, polyethylene imine

ÖZ

NİKEL/TİTANYUM KARBÜR NANOKOMPOZİTLERİN ELEKTRODEPOZİSYONU VE KARAKTERİZASYONU

Acet, Nurcan
Yüksek Lisans, Kimya Mühendisliği Bölümü
Tez Yöneticisi: Yrd. Doç. Dr. Damla Eroğlu Pala

Haziran 2017, 95 sayfa

Nikel/seramik parçacık kompozitler, yüksek sertlik ve aşınma ve korozyona karşı dayanıklılık özelliklerinden ötürü, havacılık endüstrisinde tipik olarak kullanılan krom ve kadmiyum esaslı kaplamalara çevre dostu alternatif malzemeler olarak dikkat çekmiştir. Ni/seramik parçacık kompozitlerin elektrodepozisyonu, geleneksel üretim yöntemlerine göre daha düşük işletme maliyeti ve çalışma sıcaklığı avantajlarına sahiptir. Seramik nanoparçacıkların Ni matrise inkorporasyonu, bu bileşiklerin tribolojik ve mekanik özellikleri üzerinde önemli bir etkiye sahiptir. Bununla birlikte, depozitte yüksek ve eş-dağılımlı parçacık inkorporasyonu elde etmek, elektrolit içindeki bu nanoparçacıkların dispersiyonuna büyük ölçüde bağlıdır. Bu nedenle, üstün nitelikler elde etmek için, nanoparçacıkların elektrolit içindeki topaklaşması azaltılırken, depozitteki nanoparçacık miktarı arttırılmalıdır. Fakat bu çalışmadaki en büyük zorluk parçacıkların elektrolitteki stabilizasyonunu sağlamak amacıyla kullanılan dispersantların elektrodepozisyon kinetiğini önemli ölçüde etkileyebilmesidir.

Bu çalışmanın amacı, katyonik bir dispersant olan polietilen iminin (PEI) Ni/TiC elektrodepozisyonu üzerindeki etkisini araştırmaktır. Dispersantın, parçacığın

elektrolitteki kararlılığına, depozite inkorporasyonuna ve ayrıca elektrodepozisyon kinetiğine olan etkisi araştırılmıştır. Öncelikle, PEI'nin elektrolit içindeki parçacık dağılımı üzerindeki etkisini belirlemek için zeta potansiyel ölçümleri gerçekleştirilmiştir. İkinci olarak, PEI'nin elektrodepozisyon kinetiği üzerine etkisi Lineer Süpürme Voltametri (LSV) tekniği kullanılarak ve akım verimliliği ölçümleri gerçekleştirilerek araştırılmıştır. Son olarak, nanokompozitteki TiC miktarı, Taramalı Elektron Mikroskobu/Enerji Dağılımlı X-Işını Spektroskopisi (SEM/EDS) kullanılarak analiz edilmiştir. Elektrodepozisyon kinetiğini olumsuz etkilemeden elektrolitteki parçacık dispersiyonunu iyileştiren ve nanokompozitteki TiC hacim yüzdesini arttıran optimum PEI banyo konsantrasyonu 125 ppm olarak tespit edilmiştir. Buna ek olarak, parçacık banyo konsantrasyonunun Ni/TiC elektrodepoziyonu üzerindeki etkisi karakterize edilmiş ve optimum TiC konsantrasyonu 5 g L^{-1} olarak belirlenmiştir. Ayrıca, akım yoğunluğunun Ni/TiC elektrodepozisyonuna etkisi araştırılmış ve akım yoğunluğunun artmasıyla birlikte TiC inkorporasyonunun azaldığı görülmüştür. Karıştırma hızının TiC inkorporasyonu üzerindeki etkisi de karakterize edilmiş ve en yüksek parçacık katılımının 900 rpm dönüş hızında elde edildiği saptanmıştır. Son olarak, üretilen nanokompozitler saf Ni kaplamayla mekanik ve morfolojik açılardan karşılaştırılmıştır. TiC parçacıklarının metal matristeki eş-dağılımı gözlenmiştir. Ayrıca Ni/TiC nanokompozitlerin sertliği saf Ni kaplamadan daha yüksektir.

Anahtar kelimeler: Elektrodepozisyon, Metal/seramik parçacık nanokompozit, Ni/TiC kodepozisyonu, Ni/TiC nanokompozit, dispersant, polietilen imin

To those who heartily support me at every turn,

Without whom none of my success would be possible

ACKNOWLEDGEMENTS

I would like to express my deepest appreciations to my supervisor Asst. Prof. Dr. Damla Eroğlu Pala for her great guidance, unbroken support, contributions and patience throughout my thesis. I am grateful to her for being excellent motivation source and mentor.

I would like to present my gratitude to Assoc. Prof. Dr. İrem Erel Göktepe and her student Dilara Gündoğdu for their valuable supports on zeta potential analysis. Special thanks to Dr. Gökçe Avcıoğlu for her help to learn instruments and Pine Software. I would like to thank to Electrochemical Engineering Research Team members; especially Nisa Erişen and Nurber Emerce for their partnership. I also wish to thank to METU-Central Laboratory (ODTÜ-Merlab) for zeta potential measurements, SEM/EDS analysis, nanoindentation hardness measurements.

This study was funded by The Scientific and Technological Research Council of Turkey (TÜBİTAK), Grant no: 116C005. This support is gratefully acknowledged.

I would like to present my special thanks to Zeynep Karakaş, Arzu Arslan, Atalay Çalışan, Berna Sezgin, Veysi Halvacı, Berrak Erkmen, Beril Dumanlılar and Soner Yaşar for their friendship, precious advice moral support.

Last but not the least, I want to express my sincere gratitude to my family; Hanife, İsmail and Elif Selin Acet for their unconditional love, support and encouragement in every step in my life. Finally, I would like to present my deepest thanks to Göker Akıncı who supported me all the while, in every respect.

TABLE OF CONTENTS

APPENDICES

LIST OF TABLES

LIST OF FIGURES

LIST OF SYMBOLS

Symbol	Definition	Unit
$A_p(h_c)$	Projected area of indentation at contact depth	mm^2
Ar	Residual indentation area	mm^2
E	Electrochemical potential	V
E_r	Elastic modulus	GPa
F	Faraday's constant	96485 C
H	Microhardness	HV
H_{IT}	Indentation hardness	GPa
i	Current density	mA cm^{-2}
M_n	Molar mass	g mol^{-1}
m	Mass of the substrate liberated at an electrode	g
N	Valence number	mol ion^{-1}
P_{max}	Max load	Pa
Q	Total electric charge passed through the substance	C
U	Thermodynamic equilibrium potential	V
S	Stiffness	N m^{-1}
Greek letters		
β	Geometric constant	-
ρ	Density	g cm^{-3}

LIST OF ABBREVIATIONS

AAS	Atomic absorption spectroscopy
AFM	Atomic force microscopy
BSED	Backscattered electron detector
CE	Counter electrode
DC	Direct current
EDS	Energy dispersive x-ray spectroscopy
ETD	Everhart-Thornley detector
LSV	Linear sweep voltammetry
Ni/TiC	Nickel/titanium carbide
OCP	Open circuit potential
PDC	Pulsed direct current
P	Potentiostatic
PEI	Polyethylene imine
PDC	Pulsed direct current
PP	Pulsed potentiostatic
ppm	Parts per million
PRC	Pulsed reversed current
RDE	Rotating disk electrode
RE	Reference electrode
rpm	Revolution per minute
SEM	Scanning electron microscope
vol.%	Volume percent
WE	Working electrode
XRD	X-ray diffraction

CHAPTER 1

INTRODUCTION

Chromium/cadmium coatings have been widely used in the industry for wear-resistant coatings. But due to their high degree of toxicity, their usage is planned to be restricted with environmental regulations. Thus, metal/ceramic particle composites as coatings have gained great importance in many application areas such as automotive and aerospace industries due to their high hardness and wear and corrosion resistance.

Metal/ceramic particle composites are formed by the dispersion of hard ceramic particles like aluminum oxide, silicon carbide or titanium carbide in a metal matrix such as cobalt or nickel. The metal matrix provides a compliant support for reinforcement and ceramic particles enhance mechanical properties of metal matrix. Among these metal matrix materials, nickel has certain advantages. First of all, nickel is a hard and ductile material with a high melting point. In addition, since it has a slow rate of oxidation, it can be considered as corrosion resistant. As a reinforcement material, titanium carbide is preferred due to its high melting point, high hardness, low density, high mechanical stiffness and good corrosion and wear resistance [1]. Therefore, nickel/titanium carbide (Ni/TiC) composites are good candidate, for use in automotive and aerospace industries.

Metal/ceramic particle composites as coatings have been produced by chemical vapor deposition, physical vapor deposition, plasma spraying and electrodeposition [2]. However, electrodeposition is one of the most convenient methods due to its low operating temperature and operating cost. In addition, it provides good control of the operating parameters such as thickness. Moreover, it can be applied to complex shapes with industrial applicability. Therefore, in this study, the electrodeposition of Ni/TiC nanocomposites is investigated.

Electrodeposition is a process in which metal cations in the solution are reduced and deposited on a cathode by using electrical current. For electrodeposition, three electrode system combined with a potentiostat is used. An electrode is an electrical conductor that allows the electron transfer between the anode and the cathode. These three electrodes are immersed into an electrolyte which provides ion transfer. Figure 1.1 shows the schematic representation of three electrode system.

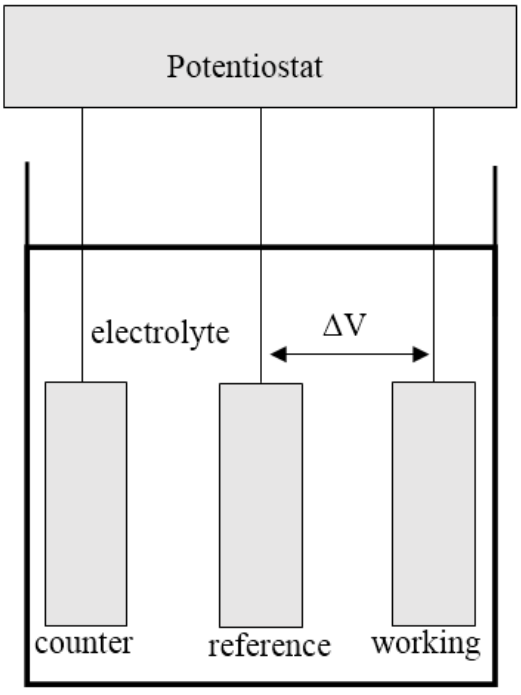

Figure 1.1 Three electrode system (adapted from [3])

In the three electrode systems, the current passes between the counter and the working electrode. The potential between the working electrode and the reference electrode is monitored [3]. In this study, Watts solution, which is a typical plating bath for nickel deposition, is used as the electrolyte. Watts solution is aqueous solution of $NiSO_4.6H_2O$ (nickel (II) sulfate hexa-hydrate), $NiCl_2.6H_2O$ (nickel (II) chloride hexa-hydrate) and H_3BO_3 (boric acid). The counter electrode is nickel at solid state, and it is used to keep nickel ion concentration of the electrolyte constant. The reference electrode is Ag/AgCl (saturated KCl) which is used to measure the potential of the working electrode relatively. The working electrode is the cathode where the nickel reduction reaction occurs. As a side reaction, hydrogen evolution reaction also takes place on the working electrode due to their similar thermodynamic potentials. The reactions and their potentials are given for a pH value of 4.4 in equations 1.1 and 1.2 [4].

$$Ni^{2+} + 2e^- \rightarrow Ni \qquad U = -0.46\,V\ vs.\,Ag/AgCl \qquad \text{Equation 1.1}$$

$$2H^+ + 2e^- \rightarrow H_2 \qquad U = -0.49\,V\ vs.\,Ag/AgCl \qquad \text{Equation 1.2}$$

The schematic of the electrodeposition process is shown in Figure 1.2. Ceramic particles, which are TiC nanoparticles for this study, are present in the electrolyte with metal ions that are Ni^{2+}. They are co-deposited on the electrode surface and form Ni/TiC nanocomposites by using electrical current. In addition to the ceramic particles and the metal ions, electrolyte may also contain dispersion and plating additives. Dispersion additives are used to inhibit the agglomeration of the ceramic particles in the electrolyte and to increase their stability. Plating additives such as 1,4-butyne diol or ethylene sulfonic acid are added to control the properties of the deposited film (brightness, roughness, etc.).

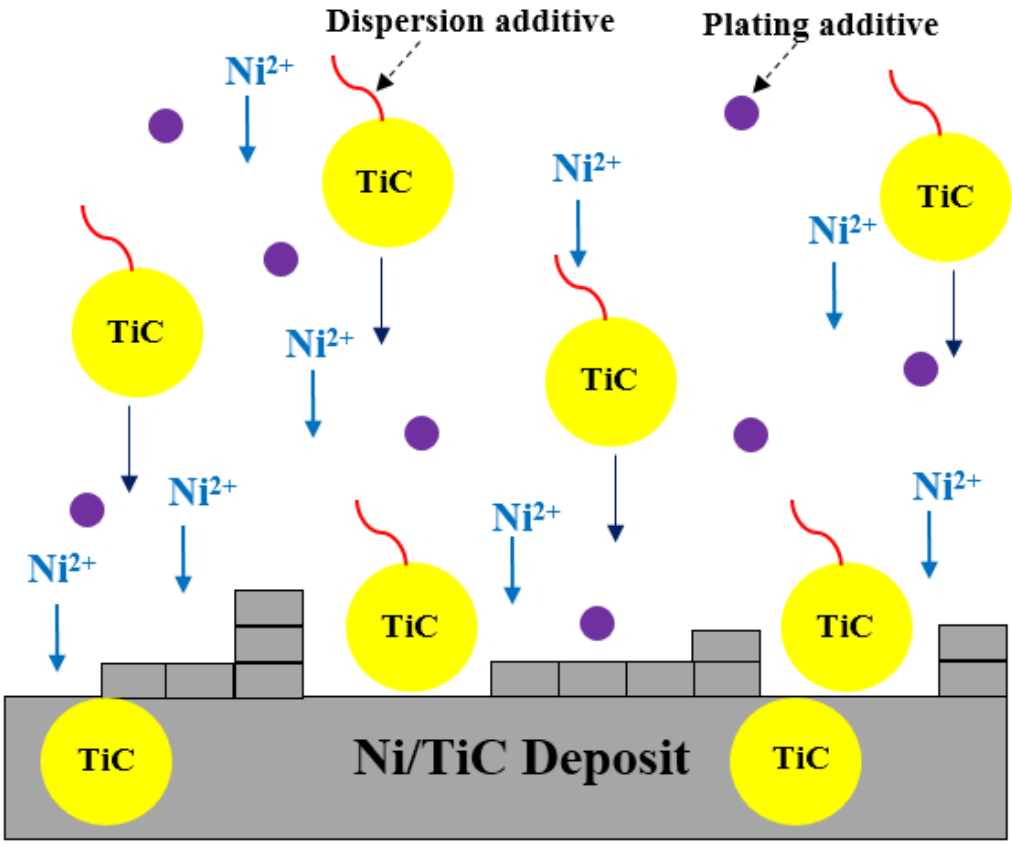

Figure 1.2 Schematic diagram of Ni/TiC electrodeposition (adapted from [5])

In order to understand the co-deposition of the metal, which has good electrical conductivity, with inert materials that are ceramic particles with poor electrical conductivity in the electrolyte, several mechanisms were proposed [6]–[14]. The transport of ceramic particles might be possible with electrophoresis, mechanical entrapment, adsorption and convective-diffusion [6]–[14]. In the model proposed by Eroglu and West [6], the co-deposition mechanism was explained in three steps. First, ceramic particles are transferred from the bulk to the electrode surface by convective-diffusion. Then, they are adsorbed on the electrode surface. Finally, the particles are incorporated into the deposit. Schematic diagram of the proposed mechanism is shown in Figure 1.3 [6].

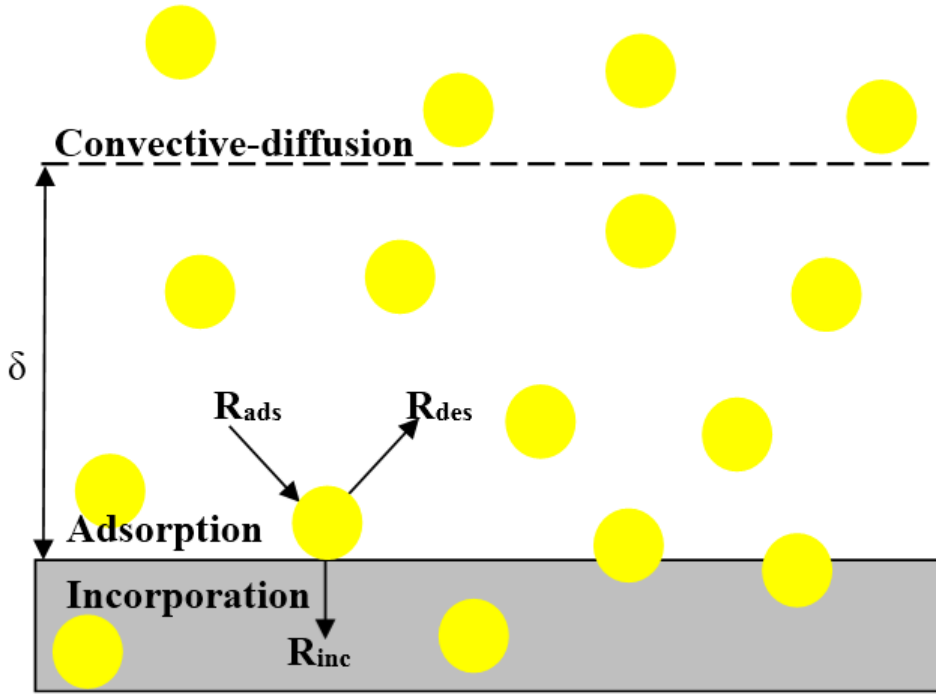

Figure 1.3 Mechanism of co-deposition (adapted from [5])

There are certain parameters that affect the electrodeposition significantly. These parameters can be divided into three main categories: ceramic particle properties, operating conditions and electrolyte composition.

The first one is the ceramic particle properties. The type of the ceramic particle such as oxide, nitride or carbides used in the electrodeposition is critical. The size of the ceramic particle (nanoparticles vs microparticles) is another important parameter. For instance, it was reported that using ceramic nanoparticles instead of microparticles results in lower incorporation of the ceramic particle into the deposit [1]. However, using ceramic nanoparticles leads to superior mechanical properties and enhanced tribological properties compared to microcomposites. The concentration of the ceramic particle in the electrolyte has a significant effect on the electrodeposition too.

The second crucial set of parameters affecting electrodeposition is the operating parameters. The operating temperature and pH influence the electrodeposition kinetics, for instance the current efficiency of the nickel deposition. In addition, increasing temperature leads to a decrease in the TiC incorporation into the deposit by aggravating TiC particle adsorbability [2]. Moreover, adjusting pH may change the surface charge of the TiC particles by adsorption of H^+ cations or OH^- anions on the surface and affects the incorporation. The electrodeposition also depends on the hydrodynamic conditions. Using rotating disk electrode for the cathode proposes good control of hydrodynamic conditions. In addition, electrodeposition technique definitely has a critical impact on electrodeposition [15]. Table 1.1 summarizes the electrodeposition techniques used in different type of processes. It is seen that direct current (DC) is a convenient method for the Ni/TiC nanoparticle electrodeposition. In DC, constant current is used. The current density is also a key parameter in the electrodeposition process.

Table 1.1 Electrodeposition techniques (adapted from [15])

Process	**Electrodeposition technique**
Deposition of metal with nanoparticles	Direct current (DC) Pulsed direct current (PDC)
Deposition of metal alloys with nanoparticles	Pulsed reversed current (PRC) Potentiostatic (P)
Multilayer deposition with nanoparticles	Pulsed potentiostatic (PP)

Finally, electrodeposition strongly depends on the electrolyte composition. The type and concentration of the dispersion/plating additives influence the electrodeposition significantly. The selection of the type of dispersion additive such as anionic or cationic is an important consideration. The addition of the dispersant to the electrolyte prevents agglomeration of the ceramic particles in the

electrolyte and enhances the stability of the particles. Thus, uniform distribution of the particles in the deposit might be achieved. Nevertheless, dispersion additives may adversely affect the electrodeposition kinetics. Therefore, the electrolyte concentration of the dispersion additive must be optimized to achieve uniform and high incorporation of TiC into the deposit without suppressing the electrodeposition. Similar considerations are also valid for plating additives. Yet, plating additives are used to control the final film properties for industrial applications; in this study, the effect of plating additives is not considered.

1.1. Scope of Current Work

In order to obtain superior mechanical, morphological and tribological composite properties, uniform and high TiC incorporation into the deposit is critical. This is only possible with high dispersion of TiC nanoparticles in the electrolyte. While the dispersion additives enhance the stability of TiC nanoparticles in the electrolyte, they may also have an adverse effect on the electrodeposition kinetics. This may be due to the adsorption of the dispersant on the surface of the electrode decreasing the active sites for the Ni/TiC co-deposition. In addition, using a dispersant might promote the hydrogen evolution, which is an undesired side reaction. This may cause hydrogen embrittlement. Hydrogen embrittlement is the phenomenon in which metals become brittle and fracture because of the diffusion of hydrogen into the metal deposit [16]. In the metal/ceramic nanocomposites, cracks might occur due to the hydrogen embrittlement and deteriorate the mechanical properties of the composite. Therefore, the major concern in the electrolyte design is attaining the optimum electrolyte concentration of the dispersant resulting in good particle stability in the electrolyte leading to high and uniform particle incorporation into the deposit without affecting the electrodeposition kinetics negatively. To obtain such a system, electrodeposition of

Ni/TiC should be investigated in terms of TiC nanoparticle dispersion in the electrolyte, electrodeposition kinetics and TiC amount in the deposit. A detailed literature survey about Ni/TiC electrodeposition is given in Chapter 2. However, there is no study that investigates the dispersion of the particles in the electrolyte, electrodeposition kinetics, particle incorporation into the deposit and the mechanical and morphological properties of the Ni/TiC nanocomposites in the presence of a dispersant. Thus, the importance of this study is the characterization of Ni/TiC electrodeposition in the presence of a dispersant in terms of all these aspects.

In this study, in order to improve the dispersion of TiC nanoparticles in the electrolyte, a cationic polymer polyethyleneimine (PEI) was used. Cationic dispersants not only enhance the stability of the particles in the electrolyte but may also improve the affinity of these ceramic particles towards the cathode [17].

The effect of PEI electrolyte concentration on the TiC particle dispersion, electrodeposition kinetics and also incorporation of TiC into the deposit was examined in this study. The effect of the cationic dispersant on the Ni/TiC electrodeposition was characterized by zeta potential analysis for investigating the particle dispersion, linear sweep voltammetry analysis and current efficiency measurements for studying the electrodeposition kinetics and SEM/EDS analysis for quantifying the TiC incorporation into deposit. The experimental methods used and results of the study are discussed in Chapters 3 and 4, respectively.

In this study, the effect of critical parameters on the electrodeposition of Ni/TiC was also characterized in the presence of the cationic dispersant. Spherical TiC nanoparticles with average diameter of 40-60 nm were used since thermal stability and hardness of metal/ceramic particle nanocomposites are known to be higher than the metal/ceramic particle microcomposites due to the prevention of dislocation movements [1]. First, the effect of electrolyte concentration of the TiC

nanoparticles were investigated. Previously, operating parameters that have an impact on the electrodeposition was summarized in five categories which are the operating temperature, pH of the electrolyte, electrodeposition technique, current density and hydrodynamics. Among these operating parameters, the effect of operating temperature and electrolyte pH were previously investigated [2], [18], [19]. For Ni/TiC electrodeposition, it was reported that the optimum operating temperature is around 50^{o}C [1], [20]–[23]. Therefore, in this study, experiments were performed at 50^{o}C. In the literature, pH of the electrolyte was commonly reported as 4.4 [1], [20]. So, pH value of Watts solution was adjusted with 1 M sodium hydroxide (NaOH) to 4.4. Electrodeposition was carried out with the DC technique. The effect of current density on Ni/TiC electrodeposition in terms of incorporation of TiC into the deposit was examined by adjusting the current density from -10 mA cm^{-2} to -100 mA cm^{-2}. In addition, the effect of hydrodynamics on Ni/TiC electrodeposition was characterized by varying the rotation speeds of the RDE. The effect of these parameters on the TiC incorporation into deposit was examined using SEM/EDS analysis. The results are shown and discussed in Chapter 4.

Finally, the produced Ni/TiC nanocomposites were characterized in terms of the morphological and mechanical properties. First of all, the selected Ni/TiC nanocomposites were compared with pure Ni coating in terms of morphological properties through SEM and Ti mapping analysis. Moreover, hardness measurements were performed to compare the selected Ni/TiC nanocomposites with pure Ni coating. Chapter 4 presents the results and discussion of the morphological and mechanical characterization.

CHAPTER 2

LITERATURE SURVEY

In this chapter, the previous studies in the literature are summarized in three main sections; studies on Ni/TiC electrodeposition, studies on Ni/ceramic particle electrodeposition in the presence of PEI and studies investigating the effect of dispersant bath concentration, particle size and bath concentration, current density and hydrodynamics on Ni/ceramic particle electrodeposition.

2.1. Previous Studies on Ni/TiC Electrodeposition

Although, there are many studies on ceramic particle incorporation, there are only 8 studies focusing on the electrodeposition of Ni/TiC composites specifically. These studies are summarized below chronologically.

Asadi et al. [20] used TiC particles with a diameter of 39 μm, 85 μm and 99 μm. Among them TiC particles with a diameter of 39 μm and 85 μm were produced by the combustion synthesis method. And, TiC particles with a diameter of 99 μm were purchased. These TiC particles were characterized by X-Ray Diffraction

(XRD) analysis for determination of the purity of the particles. For the Ni/TiC co-deposition, a Watts bath with a pH of 4.4 and temperature of 50°C containing 20 g L^{-1} TiC was used as the electrolyte. The electrolyte was stirred using a magnetic stirrer at 1000 rpm for 80 min. The electrodeposition was conducted at a current density of -70 mA cm^{-2} for 20 min using DC. Asadi et al. [20] stated that XRD confirms the purity of the produced TiC particles. According to the X-Ray Photoelectron Spectroscopy (XPS) results, TiO_2 was detected on the surface of the TiC particles. TiC particles' isoelectric point, which is the pH value where zeta potential value is zero, was reported as 3.3. By using isoelectric point, it was concluded that the adsorption of hydrogen complexes and intermediates might cover the active sites for electrodeposition and inhibits grain growth and forms nanoscale grain sizes which were calculated between 9 and 30 nm. SEM/EDS were utilized and TiC volume percentages in the deposit were reported as 7%, 39% and 48% for composites obtained from 99 μm (purchased), 85 μm (synthesized) and 39 μm (ball milled) particles, respectively. The microhardness of the composite produced from 99 μm TiC (purchased) was reported as 235 HV. Asadi et al. [20] stated that using magnetic stirring enhances the transport of the TiC particles in the electrolyte. Moreover, it was reported that finer particles improve the incorporation of TiC particles and lead to more uniform distribution.

Although aqueous solutions are safer, more environmentally friendly and more suitable for industrial applications, Singh and Singh [19] used N-methylformamide bath at different temperatures between 20°C and 80°C in order to prevent hydrogen evolution. TiC particles with a diameter of 4 μm were used at an electrolyte concentration between 5 g L^{-1} and 40 g L^{-1}. The electrolyte was stirred for 4 h and sonicated for 4 h before the experiment and the optimum stirring rate was reported as 750 rpm by observing the dispersion of TiC particles. The effect of particle electrolyte concentration (5 g L^{-1} - 40 g L^{-1}) and current density (-10 mA cm^{-2} to -50 mA cm^{-2}) on TiC incorporation into the deposit were examined under DC. It

was reported that increasing TiC bath concentration increases the TiC incorporation except for particle bath concentration of 20 g L^{-1} at 60ºC. Moreover, increasing current density enhances TiC incorporation up to -20 mA cm^{-2}, forms a maximum there and then decreases with increasing current density. Such a trend was explained that at low current densities, the required time for TiC encapsulation was not reached due to slow Ni deposition rate. Above the optimum current density, Ni deposition becomes too fast so that the incorporation of the particle into the growing film becomes negligible. In addition, by utilizing SEM and XRD, it was concluded that crystalline size is inversely proportional with the current density. Microhardness of pure Ni coating and composite produced with optimum conditions (60ºC, 40 g L^{-1} TiC, -30 mA cm^{-2} current density, 750 rpm rotation speed) were measured and reported as 150 HV and 220 HV, respectively. By AAS, hydrogen amount in the composite was measured around 4.5 ppm, which is quite low. Yet, crack formations at current densities greater than -30 mA cm^{-2} were revealed.

Singh et al. [18] characterized the Ni/TiC electrodeposition from a N-methylformamide bath in terms of the electrolyte temperature and current density using SEM, XRD, EDS and microhardness measurements. TiC particles smaller than 200 nm were used in the study. The optimum electrolyte temperature was reported as 60 ± 5ºC based on the quality of the nanocomposite. The optimum stirring rate was 750 rpm for sufficient agitation of particles in the electrolyte. At a current density of -30 mA cm^{-2}, the average grain size was determined between 209 nm and 738 nm with an agglomeration size of 1.4 μm. XRD results showed a shift from (111) to (110) plane when pure Ni and Ni/TiC nanocomposite were compared. According to the EDS results, increasing current density from -10 to -30 mA cm^{-2} increased TiC amount in the deposit up to 33.6 vol.%. Further increase in the current density results in a decrease at the TiC incorporation. Moreover, in order to characterize the effect of TiC bath concentration on TiC vol.% in the

deposit, electrolytes containing 10 g L^{-1}, 20 g L^{-1} and 30 g L^{-1} TiC were prepared and electrodeposition was performed. The optimum TiC concentration was determined as 20 g L^{-1} corresponding to 33.6 vol.% TiC in the deposit. In addition, microhardness of the nanocomposites, which were produced at 60^{o}C electrolyte temperature, 750 rpm stirring rate and 20 g L^{-1} TiC electrolyte concentration, were measured with respect to varying current density from -10 to -50 mA cm^{-2}. It was stated that microhardness of the Ni/TiC composites were constant around 180-185 HV up to -30 mA cm^{-2}. At higher current densities microhardness sharply increases to 210-215 HV. Yet, the trend was unexpected. The hardness of the annealed nanocomposite dropped to 90 HV. High annealing temperature of 800^{o}C might lead to strain release from the nanocomposite.

Karbasi et al. [1] used 50 nm – 200 nm TiC nanoparticles in a Watts bath with constant particle electrolyte concentration of 6 g L^{-1}. The electrolyte was stirred at 250 rpm for at least 12 h and sonicated for 20 min before co-deposition. Temperature and pH of the electrolyte were kept constant at 50^{o}C and 4.4, respectively. During co-deposition argon gas was fed from the cell bottom in order to stir the electrolyte. Electrodeposition was performed for different current densities between -20 mA cm^{-2} and -150 mA cm^{-2} under DC in order to examine the effect of current density on the nanocomposite properties such as the TiC vol.%, microhardness, grain size and % dislocation. SEM and EDS were utilized to characterize the structure, morphology and thickness of the nanocomposite film and TiC incorporation into the deposit at a magnification of x5000. XRD and Vickers microhardness measurements were used to evaluate phase and microhardness of the nanocomposite, respectively. XRD analysis showed that at all current densities, produced nanocomposites have peaks corresponding to the TiC phase. While up to a current density of -70 mA cm^{-2} TiC peaks becomes stronger, further increase in the current density results in a decline of peaks corresponding to the TiC. Furthermore, microhardness and TiC vol.% in the

deposit presented similar trends, showing a maximum at 410 HV and 11.8%, respectively at a current density of -70 mA cm^{-2}. This trend was explained by Gugliemi's transport model [7], which explains the co-deposition at 2 stages. First stage is the weak adsorption of the particles onto the cathode due to van der Waals force. In the second step, the particles are adsorbed strongly and irreversibly into the deposit due to electrostatic force between the particles and adsorbed anions. To conclude, it was stated that at low current densities, transport of Ni ions to the cathode surface has such a low rate that time required for the adsorption of the particles is not sufficient. Thus, low incorporation of TiC into the deposit was achieved at low current densities. On the other hand, higher current densities lead to much faster transport of Ni ions from the anode to the cathode than the transport of particles from bulk to the cathode surface by mechanical stirring. And such phenomena result in low incorporation and thus low microhardness. It was reported that the particle incorporation into the deposit decreases the grain size of the deposit. Thus, dislocation movements decrease. Therefore, microhardness of Ni/TiC composites are higher than pure Ni coatings. Moreover, Ti mapping was performed for pure Ni and the nanocomposite produced with the optimum conditions. By this method, uniform dispersion of TiC into deposit was claimed.

Raja et al. [2] also used Watts bath with 50-100 nm TiC nanoparticles. TiC electrolyte concentration, electrolyte temperature and pH were changed from 2 g L^{-1} to 15 g L^{-1}, 30^{o}C to 60^{o}C and 2 to 5, respectively. The electrodeposition was performed under DC for current densities of -20 mA cm^{-2} to -100 mA cm^{-2}. Raja et al. used a dispersant, sodium lauryl sulfate, with a constant electrolyte concentration of 50 ppm. During co-deposition, magnetic stirring was provided. SEM, XRD, Vickers microhardness measurement, chronopotentiometry and electrochemical impedance spectroscopy (EIS) were used for the characterization of Ni/TiC electrodeposition. The optimum TiC bath concentration was determined as 8 g L^{-1} corresponding to the maximum TiC vol.% in the deposit. Higher particle

concentrations resulted in agglomerations of TiC and lowered the incorporation of TiC into the nanocomposite. The maximum incorporation of TiC into the deposit based on volume was 10.8% for an electrolyte temperature of 50ºC, pH of 4, TiC electrolyte concentration of 8 g L^{-1} and current density of -80 mA cm^{-2}. Increasing the current density up to -80 mA cm^{-2} resulted in increasing TiC incorporation whereas further increase in the current density leads to a decrease in the TiC amount. Raja et al. explained such a trend due to the fact that nickel cations might be reduced under concentration over potential and hydrogen evolution reaction may be enhanced. However, Raja et al. did not study Ni/TiC electrodeposition in terms of the electrodeposition kinetics. pH and temperature of the electrolyte were optimum at 4.4 and 50ºC, respectively. Higher pH resulted in a brittle nanocomposite under conditions of 8 g L^{-1} particle bath concentration and -80 mA cm^{-2}. Temperatures greater than 50ºC caused low incorporation due to the increase in the kinetic energy of the particles and difficulties of adsorption of particles into the growing film. The adhesion of the nanocomposite to the steel cathode as substrate was also tested by bending test and good adhesion was reported. According to the SEM images, uniform particle distribution due to the dispersant was claimed. Increasing TiC vol.% in the nanocomposite were validated by XRD analysis. Using Debye–Scherrer equation, the average grain sizes for pure Ni and nanocomposite produced with optimum conditions were calculated as 31 nm and 17 nm respectively. Furthermore, microhardness was measured as 320 HV for pure Ni and 400 to 525 HV for nanocomposites. Corrosion resistance of the nanocomposites has been enhanced with increasing TiC amount in the deposit; increasing semicircle diameter of the Nyquist plot indicates more inert coatings [24].

Yang et al. [21] used Watts bath containing TiC microparticles with a diameter of 2 μm and nanoparticles with a diameter of 200 nm. In this study, similar to Raja et al. [2], Sodium lauryl sulfate was used as a dispersant with a high concentration of

200 g L^{-1}. Electrodeposition temperature, stirring rate and current density were 50°C – 60°C, 300 rpm and -20 mA cm^{-2}, respectively. AFM was utilized for topographical information. In order to investigate the corrosion behavior, open circuit potential (OCP) in NaCl solution was plotted against time. Electron work function, which is the minimum energy required to move electrons at Fermi level inside a metal to its surface without kinetic energy [25], was used to investigate the corrosion behavior of metals [26] and Ni/SiC composites [27]. Electron localization function was calculated for better understanding of bond strength at the Ni/TiC interface. Random distribution of TiC in the microcomposites was reported whereas uniform distribution of TiC in the deposit for composites produced from TiC nanoparticles were observed. In addition, using nanoparticles resulted in higher OCP which corresponds to higher corrosion resistance when compared to pure Ni coating. On the contrary, microparticle addition caused lower corrosion resistance than pure Ni coating. Electron work function results also confirmed that the nanocomposites have higher Electron work function compared to pure Ni and microcomposites. Therefore, the lowest corrosion tendency due to stronger interfacial bonding was reported for the Ni/TiC nanocomposite. It was stated that, Ni/TiC interface had either poor bond or no bond for composites produced from TiC microparticles.

Danaila et al. [22] utilized Watts bath as the electrolyte with a constant temperature at 50°C, pH of 4.04 and TiC nanoparticles with an average diameter of 50 nm. TiC electrolyte concentration was 10 g L^{-1}. The electrolyte was stirred magnetically. Electrodeposition was performed at constant current at both -40 mA cm^{-2} and -72 mA cm^{-2}. SEM, thickness measurements, EDS, XRD, surface roughness measurements, nanoindentation hardness measurements and fretting wear tests under wet condition were performed for characterization. SEM images given in Figure 2.1 and Figure 2.2 show pyramidal structure for pure Ni coating and cauliflower structure for Ni/TiC composite.

Pyramidal structure for pure Ni coating and cauliflower structure for nanocomposites composite were already reported in the previous studies [28], [29]. The maximum TiC vol.% in the deposit was stated as 10.34% at -40 mA cm^{-2}. XRD also confirmed the TiC incorporation into the deposit. Roughness of pure Ni coating and Ni/TiC nanocomposites were reported 50.60 nm and 217.69 nm, respectively by using non-contact white light interferometry. It was concluded that cauliflower structure obtained due to the TiC incorporation into the growing film increases the surface roughness. Coating thicknesses for pure Ni and Ni/TiC nanocomposite were above 10 μm. Nanoindentation hardness were reported as 3.64 GPa for pure Ni and 4.32 GPa for Ni/TiC nanocomposite. According to the OCP measurement results, Ni/TiC nanocomposites had higher OCP than pure Ni coating showing higher corrosion resistance. Moreover, the friction coefficient of the Ni/TiC nanocomposite was also lower than the friction coefficient of pure Ni coating.

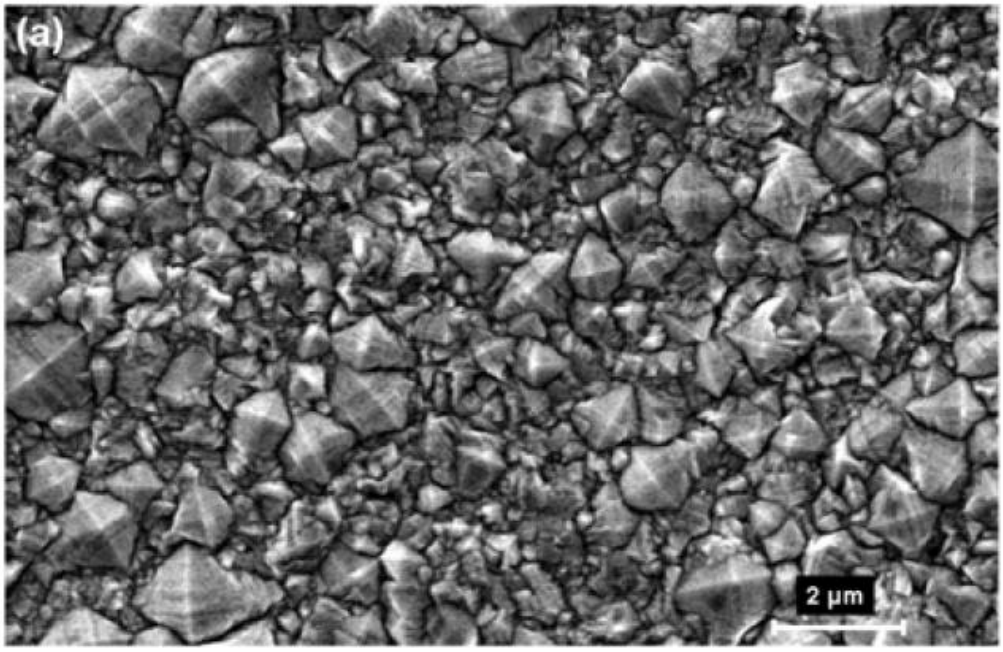

Figure 2.1 Pyramidal structure of pure Ni coating (adapted from [22] with permission)

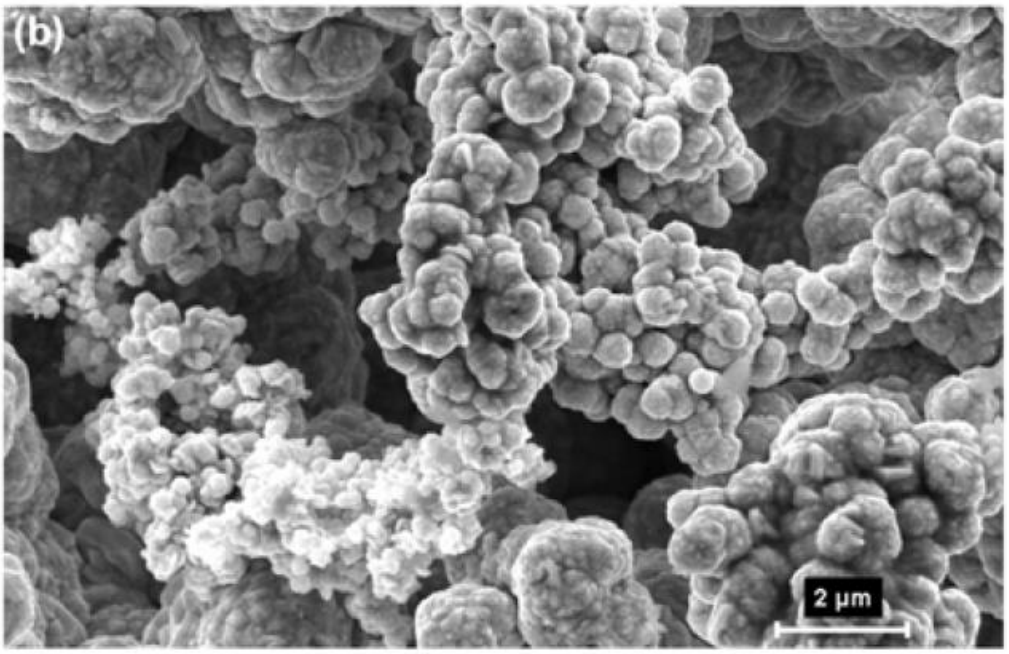

Figure 2.2 Cauliflower structure of Ni/TiC nanocomposite (adapted from [22] with permission)

Benea et al. [23] used similar experimental setup and parameters to Danaila et al. [22] in terms of the electrolyte type, pH, temperature, TiC size and electrolyte concentration and current density. In this study, SEM, EDS, XRD, thickness, surface roughness and nanoindentation hardness measurements and fretting wear tests under dry condition using reciprocating ball-on-disk computer-controlled tribotester were performed for characterization. Similar to the previous studies, pyramidal structure for Ni coating and cauliflower structure for Ni/TiC composite were observed. The maximum TiC vol.% in the deposit was reported as 8.68% with operating conditions which are pH value of 4.4, electrolyte temperature of 50 ^{o}C, TiC electrolyte concentration of 10 g L^{-1} and current density of -40 mA cm^{-2}. Roughness of Ni coating and Ni/TiC nanocomposite were stated as 50.6 nm and 192.99 nm, respectively. According to the nanoindentation results, hardness of

Ni/TiC nanocomposite reported as 4.32 GPa was higher than Ni coating reported as 3.64 GPa. The friction coefficients with respect to normal force were stated for both Ni coating and Ni/TiC nanocomposites under dry condition by using tribotester. For all normal forces between 1 N and 5 N and fretting frequencies between 1 Hz and 5 Hz, nanocomposites showed lower friction coefficient than Ni coating. So, it can be inferred that Ni/TiC nanocomposite has higher mechanical and tribological resistance than Ni coating. SEM analysis after the fretting wear test showed smaller wear track for the composites than the one for pure Ni. Moreover, by utilizing EDS around wear tracks, it was concluded that oxidation enhances delamination of wear particles which was also reported by Vieira et al. [30].

The previous studies on the Ni/TiC electrodeposition are summarized in Tables 2.1 and 2.2. These tables give important parameters in terms of the particle characteristics, operating conditions and electrolyte type and composition. TiC incorporation in terms of TiC volume fraction in the deposit is also presented. To conclude, the effect of dispersant electrolyte concentration on Ni/TiC electrodeposition was not characterized in the literature before in terms of the dispersion of particles in the electrolyte, electrochemical kinetics, particle incorporation and mechanical and morphological properties of Ni/TiC composites as shown in Tables 2.1 and 2.2.

Table 2.1 Previous studies in the literature focusing on Ni/TiC electrodeposition

Parameters / Author	**Asadi et al** [20]	**Singh and Singh** [19]	**Singh et al** [18]	**Karbasi et al** [1]
Electrolyte Type	Watts soln	N-methylformamide	N-methylformamide	Watts soln
Temperature (ºC)	50	20-80	20-80	50
pH	4.4	-	-	4.4
Particle Size (µm)	99-85-39	<4	<0.2	0.05-0.2
Current Density (mA cm^{-2})	70	10-50	5-70	20-150
Current Type	DC	DC	DC	DC
Rotation Speed (rpm)	1000	200-1200	200-1200	250
TiC Electrolyte Concentration (g L^{-1})	20	5-40	10-30	6
Dispersant Type	-	-	-	-
Dispersant Electrolyte Concentration (ppm)	-	-	-	-
TiC vol. % in the Deposit (%)	7.04-38.96-48.45	23.72	33.57	11.80
Microhardness (HV)	235	220	180-185, 210-215	410

Table 2.2 Previous studies in the literature focusing on Ni/TiC electrodeposition

Parameters / Author	**Raja et al** [2]	**Yang et al** [21]	**Danaila et al** [22]	**Benea et al** [23]
Electrolyte Type	Watts soln	Watts soln	Watts soln	Watts soln
Temperature (°C)	30-60	50-60	45	45
pH	2-5	-	4.04	4.04
Particle Size (µm)	0.05-0.1	0.2-2	0.05	0.05
Current Density (mA cm^{-2})	20-100	20	40-72	40-72
Current Type	DC	DC	DC	DC
Rotation Speed (rpm)	-	300	-	-
TiC Electrolyte Concentration (g L^{-1})	2-15	-	10	10
Dispersant Type	Sodium lauryl sulfate	Sodium lauryl sulfate	-	-
Dispersant Electrolyte Concentration (ppm)	50	200,000	-	-
TiC vol. % in the Deposit (%)	10.80	-	10.34	8.68
Microhardness (HV)	400-525	-	400	400

2.2. Previous Studies on Ni/Ceramic Particle Electrodeposition in the Presence of PEI

Polyethylene imine (PEI) is a positively charged branched polymer. The chemical structure is shown in Figure 2.3.

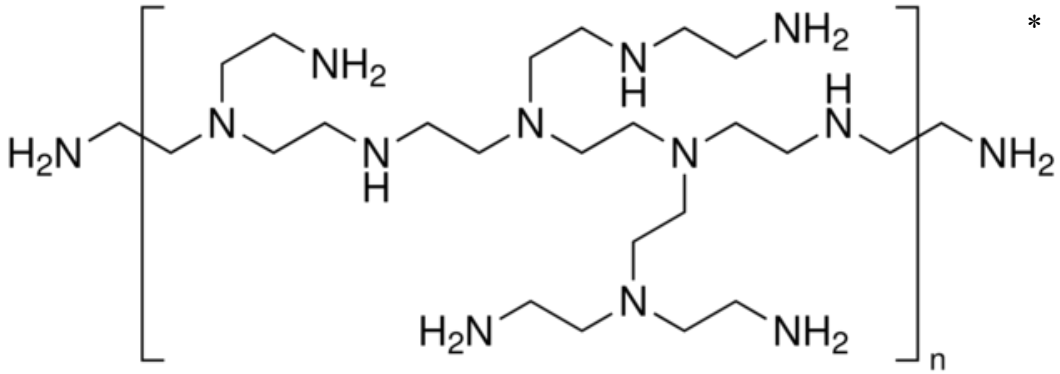

* PEI has at least 1 protonated nitrogen in the solution

Figure 2.3 The chemical structure of PEI [31]

PEI is commonly used for ceramic colloidal systems in order to enhance dispersion [31]. In the literature, there are some studies which investigate dispersion and stability of silicon carbide (SiC), tungsten carbide (WC), titanium nitride (TiN) and titanium carbide (TiC) particles in aqueous media with the addition of PEI [32]–[37]. Moreover, PEI is also used as a suppressor for electrodeposition of Cu and Ni [38], [39]. Furthermore, it was reported that PEI is an effective dispersant for Ni/SiC electrodeposition [40], [41].

2.2.1. Previous Studies on the Dispersion of Ceramic Particles in Aqueous Media in the Presence of PEI

Previously, the dispersion of SiC with PEI was investigated [32]–[34]. Sun et al. [32] stated that the addition of PEI-H^+ into aqueous SiC suspension increases the surface charge of particles at a pH value of 3.57. Zhang et al. [33] showed that PEI

increased the zeta potential of SiC particles in the aqueous solution and shifted isoelectric point from 2.4 to 10.5 and resulted in well-stabilized suspensions. Zhang et al. [34] studied the effect of PEI on SiC-Al_2O_3 co-dispersion in aqueous media and concluded that PEI provides a stronger electrosteric interaction with SiC and shows superior dispersion.

Zhang et al. [35] also examined the effect of PEI on the dispersion of TiN in aqueous solution and showed that PEI is an effective dispersant for TiN as well. Laarz et al. [36] studied the dispersion of WC in the presence of PEI at aqueous medium and concluded that PEI is an efficient dispersant for such a suspension. Foratirad et al. [37] investigated the dispersion of TiC aqueous suspension with PEI by performing sedimentation, zeta potential and viscosity measurements with varying PEI concentrations. The sedimentation results are shown in Figure 2.4.

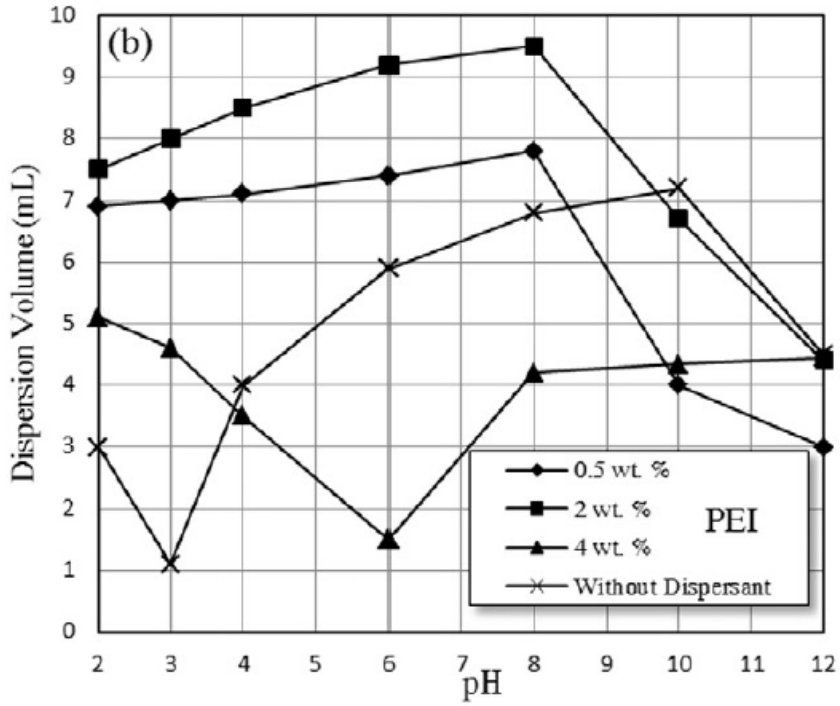

Figure 2.4 Dispersion volume with respect to pH for different PEI concentrations (adapted from [37] with permission)

According to Figure 2.4, using PEI even at low concentrations enhanced the dispersion of the suspension. Moreover, it was reported that up to 2 wt.%, PEI addition decreases the sediment volume enhancing the stability especially for pH values smaller than 8. PEI addition also resulted in highly positive zeta potential values over a wide pH range. Especially for PEI concentrations smaller than 2 wt.%, adsorption of PEI on the TiC surface increased with increasing PEI concentration. It was concluded that PEI enhances the stability of the suspension significantly.

2.2.2. Previous Studies on Metal/Ceramic Particle Electrodeposition in the Presence of PEI

Kim et al. [38] investigated the effect of PEI on Cu electrodeposition. It was stated that PEI is highly effective for suppression of Cu electrodeposition even at low concentrations such as 0.05 μmol L^{-1} due to the adsorption of PEI on the electrode surface. Kim et al. [39] also studied the effect of PEI on Ni electrodeposition. Similar to their previous work, PEI addition inhibited Ni electrodeposition. Therefore, it can be concluded that PEI can be used as a suppressor for Ni electrodeposition too.

Eroglu et al. [40] investigated the effect of PEI on both electrolyte stability, electrochemical kinetics and SiC (d = 1μm) incorporation for Ni/SiC electrodeposition. In this study, PEI with a molecular weight (M_n) of 1200 and 60000 were used with changing PEI concentrations from 0 to 1000 ppm. According to the polarization curves obtained by the LSV technique, the PEI-60000 addition up to 200 ppm did not lead to a significant inhibition. Current efficiency measurements showed that concentrations of PEI-60000 higher than 200 ppm sharply decreased the current efficiency. The effect of PEI-60000 electrolyte concentration on the incorporation of SiC was investigated and the results are

shown in Figure 2.5. SiC vol.% in the deposit increased significantly with PEI addition of 200 ppm. However, the addition PEI-60000 up to 500 ppm did not provide a significant improvement on the particle stability according to the settled volume measurements after 3 min. In order to increase the particle dispersion without suppressing the Ni deposition, a novel precoating method for the SiC particles have been developed. Zeta potential results showed that zeta potential of SiC particles increased from 6.4 mV to 60.8 mV with the pre-coating procedure. In addition, the suppression on nickel deposition was prevented. It was concluded that PEI-60000 is an effective dispersant for Ni/SiC electrodeposition.

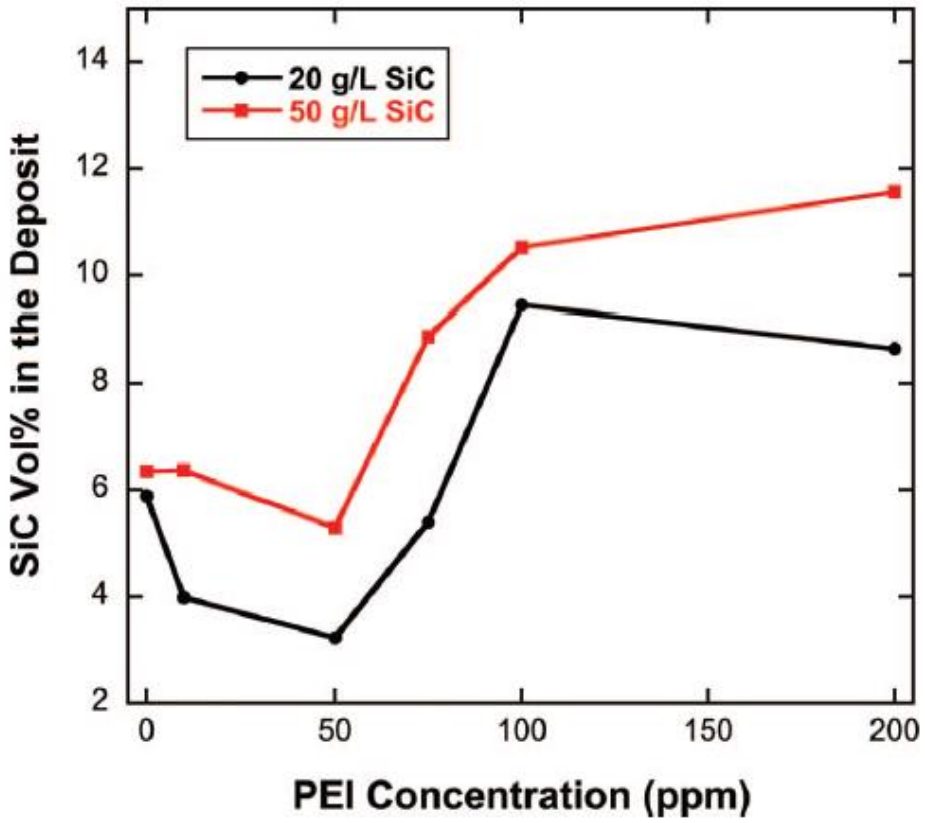

Figure 2.5 SiC content of the deposit with respect to PEI-60000 concentration (adapted from [40] with permission)

Eroglu et al. [41] also studied the effect of PEI on the electrodeposition of Ni/SiC nanocomposites containing SiC nanoparticles with a diameter of 45-55 nm. It was concluded that PEI increases the stability of SiC particles in the electrolyte with high long-term efficacy. Thus, high incorporation of SiC into the deposit was achieved with sufficiently high current efficiencies.

Vilinska et al [42] examined the dispersion of SiC micro and nanoparticles in the Watts bath at a pH of 3.5 by using settled volume analysis and absorption analysis. It was concluded that using PEI with a M_n of 60000 improves the dispersion of SiC micro and nanoparticles in the Watts bath significantly.

To sum up, PEI has been reported as a highly effective dispersant for Ni/SiC electrodeposition since both dispersion of SiC particles in the electrolyte and SiC incorporation into the deposit were enhanced in the presence of PEI [40]–[42]. Therefore, PEI might be an effective dispersant for the Ni/TiC electrodeposition too in terms of these aspects. Thus, PEI is selected as the cationic dispersant in this study.

2.3. Previous Studies Investigating the Effect of Important Parameters on Ni/Ceramic Particle Electrodeposition

The electrodeposition process and so the ceramic particle content of the deposit strongly depend on the ceramic particle properties in terms of type, size, surface properties and concentration, the operating parameters in terms of current density, temperature, hydrodynamic conditions and electrodeposition technique and plating bath properties in terms of electrolyte type, concentration, pH, dispersion and plating additives [6], [18]–[20], [40], [41]. Thus, there are several studies in the literature focusing on the effect of these parameters on the Ni/ceramic particle electrodeposition [1], [2], [6], [15], [18]–[20], [40], [41], [43]–[45].

The type and concentration of the dispersant added in order to increase the stability of the ceramic particles in the electrolyte plays a critical role in the electrodeposition of these composites [2], [6], [15], [26], [40], [41], [43]–[45]. As noted earlier, increasing the stability of the particles in the electrolyte provides a greater amount of the ceramic particles in the deposit [6], [40], [41]. Cationic additives both inhibit the agglomeration of the ceramic particles in the electrolyte and increase the tendency of the particles towards the cathode by introducing more positively charged ceramic particles [6], [40], [41]. Vilinska et al. have shown that PEI, a cationic polymer, is very effective in enhancing the stability of both SiC micro and nanoparticles [42]. Foratirad et al. presented that PEI enhances the dispersion of TiC in aqueous suspensions [37], [46]. Eroglu et al. also stated that using PEI increases the amount of SiC in the deposit significantly for both micro and nanocomposites [40], [41]. One of the most critical problems encountered in metal/ceramic particle electrodeposition is that adsorption of the added dispersant to improve the stability of the particles in the electrolyte can negatively affect the resulting electrodeposition kinetics [19], [40], [41]. Furthermore, adsorption of PEI on electrode can seriously degrade the current efficiency of the electrodeposition by increasing hydrogen evolution side reaction [19], [40], [41]. For this reason, a research methodology that considers both particle dispersion and electrodeposition is required [40], [41]. In the literature, there is no such a study investigating the effect of PEI addition on the particle stability in the electrolyte, and thus on the TiC amount in the deposit, as well as on the electrodeposition kinetics for Ni/TiC electrodeposition.

The size of the ceramic particle in the deposit is very important in terms of its composite properties [1], [2], [6], [15], [19], [41], [43]–[45]. Nanoparticle composites exhibit superior mechanical and tribological properties compared to microparticulate composites [1], [2], [6], [15], [19], [21], [41], [43]–[45]. However, when nanoparticles are used, lower ceramic particle ratios are obtained

in the deposit. For this reason, it is necessary to prevent the agglomeration of nanoparticles in the electrolyte and to increase the incorporation of particles into the deposit in order to obtain nanocomposites with superior properties [1], [2], [6], [15], [19], [41], [43]–[45].

The concentration of ceramic particles in the plating bath is one of the most studied parameters in the literature [2], [6], [15], [19], [40], [41], [43], [45]. These studies have shown that ceramic particle content in the deposit increases up to a certain point with increasing particle electrolyte concentration but the amount of ceramic particle in the composite does not depend on increasing electrolyte concentration after this point [2], [6], [15], [40], [41], [43], [45].

Another parameter that is frequently studied in the literature is the current density [1], [2], [6], [15], [19], [22], [23], [40], [41], [43], [45]. However, it is not possible to arrive at a general conclusion since the effect of current density on amount of the particles in the deposit depends on other parameters such as particle type and size and hydrodynamic conditions.

The effect of rotation speed on the ceramic particle content in the deposit is also significant [6], [15], [19], [40], [44]. According to the literature, the ceramic particle incorporation into the deposit increases with increasing mixing speed up to an optimum value, after that the increasing mixing speed reduces the ceramic particle content of composite [6], [15], [19], [40], [44]. Since particle electrolyte concentration, current density and rotation speed play a key role on the co-deposition of Ni/ceramic particle composites, characterization of Ni/TiC electrodeposition in the presence of PEI in terms of these critical parameters has a great importance for the literature.

CHAPTER 3

EXPERIMENTAL

This section summarizes the materials used for the electrodeposition of Ni/TiC nanocomposites, electrodeposition process and characterization of Ni/TiC electrodeposition.

3.1. Materials

In order to produce Ni/TiC nanocomposites, various chemicals and materials were used. Nanocomposites were composed of Ni (nickel) and TiC (titanium carbide). The electrolyte was an aqueous solution of $NiSO_4.6H_2O$ (nickel (II) sulfate hexa-hydrate, Sigma-Aldrich, 99%), $NiCl_2.6H_2O$ (nickel (II) chloride hexa-hydrate, Sigma-Aldrich, ≥ 98.5%) and H_3BO_3 (boric acid, Sigma-Aldrich, ≥ 99.5%). As a dispersion additive, $(C_2H_5N)_n$ (polyethylene imine) was used. As substrate, either Pt (Platinum) or brass was used. In addition, for chemical cleaning of substrate 0.5 M H_2SO_4 (sulfuric acid, Fluka, 95-97%) was used.

Titanium carbide was used as the reinforcement material and was procured from Nanografi Nano Technology. Tables 3.1 and 3.2 give the properties and chemical analysis data of TiC, respectively. Figure 3.1 is the SEM image of TiC which was obtained from the supplier [47].

Table 3.1 The properties of TiC [47]

Property	**Value**
Molecular formula	TiC
Purity	> 99 %
Particle size (APS)	40-60 nm
Specific surface area	> 50 m^2/g
Color	Black
Morphology	Nearly spherical
Bulk density	~0.08 g/cm^3
True density*	4.93 g/cm^3
Melting point	3200 ^oC
Crystal phase	Cubic
Zeta potential	25 V

*True density is density of solid excluding all the voids.

Table 3.2 Chemical analysis data of TiC [47]

Compounds	**Amount, wt. %**
O	< 0.9 %
Mg	< 3 ppm
Al	< 60 ppm
Cu	< 40 ppm
Si	< 35 ppm
Fe	< 5.5 ppm
TiC	> 99 %

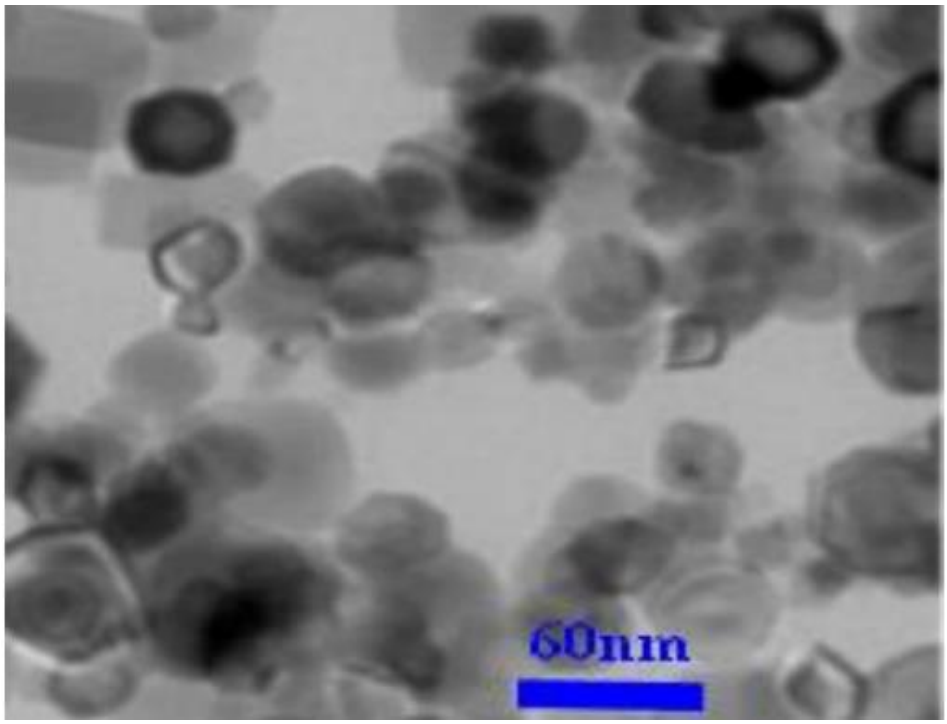

Figure 3.1 SEM image of TiC [47]

In order to improve the stability of TiC particles in the electrolyte polyethylene imine (PEI) was used as a cationic dispersant. PEI was ordered from Sigma-Aldrich. The properties of PEI are shown in Table 3.3.

Table 3.3 The properties of PEI [48]

Property	**Value**
Molecular formula	$(C_2H_5N)_n$
Number average molecular weight (M_n)	~60,000
Weight average molecular weight (M_n)	~750,000
Purity	50 wt. % in H_2O
Viscosity	18,000 – 40,000 mPa.s

Three electrode system was used for the co-deposition of Ni/TiC. These electrodes are the rotating disk electrode (RDE), the counter electrode and the reference electrode. RDE type of a working electrode, which is shown in Figure 3.2, is commonly used in the literature since it provides stirring of the fluid [49]. Thus, the transfer of the ceramic particles from the bulk to the electrode surface is enhanced. Moreover, it has advantage of good control of mass transfer conditions. It also provides reproducible fluid flow [4]. In addition, uniform current density on the electrode surface is achieved under mass-transfer limited conditions [50] .

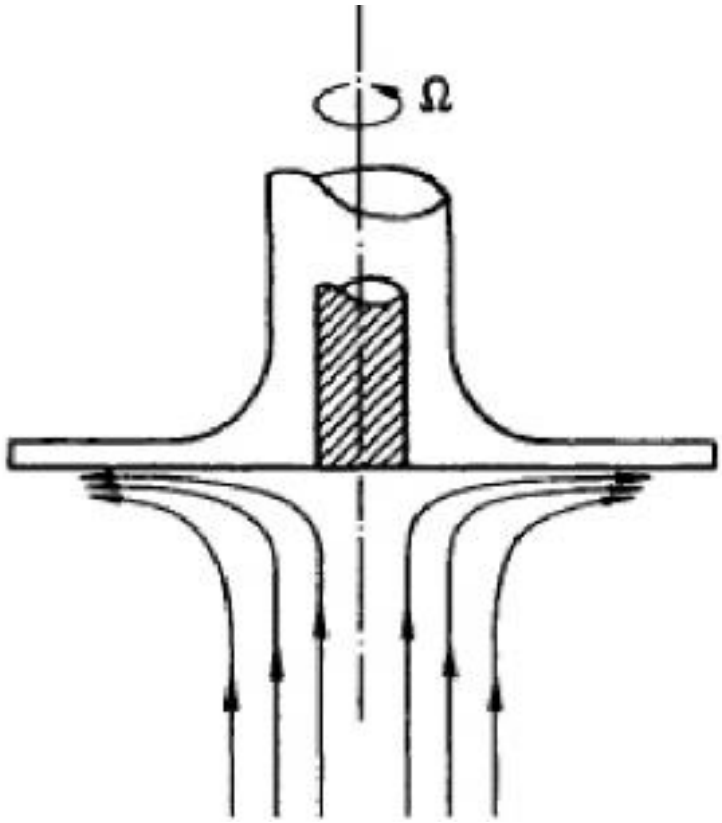

Figure 3.2 Schematic representation of RDE [49]

In this study, RDE was either platinum (Pt) or brass. Pt-RDE was purchased from Pine Research Instrumentation. Table 3.4 gives the properties of platinum rotating disk electrode. Figure 3.3 shows schematic of Pt-RDE.

Table 3.4 The properties of Pt-RDE [51]

Property	Value
Model	AFE5T050PTPK
Disk diameter	5.0 mm
Shroud diameter	15.0 mm
Tip shroud length	25.4 mm
Maximum immersion	12.0 mm
Maximum rotation rate	3000 rpm
Temperature range	10 – 80°C

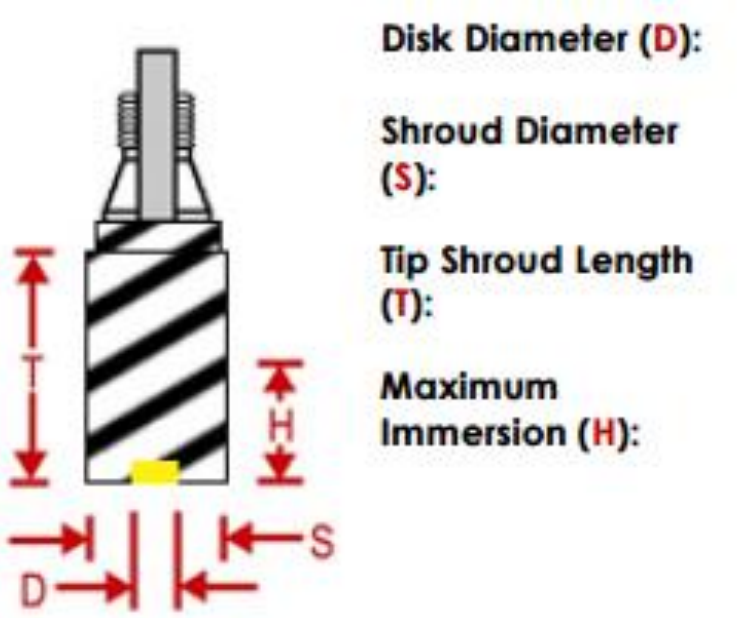

Figure 3.3 The schematic of Pt-RDE [51]

Brass rotating disk electrode was designed for applications such as SEM/EDS and hardness measurements to be able to place deposit into the instrument. Brass was purchased from Alfa Aesar. The properties of brass electrode are given in Table 3.5 and it is shown in Figure 3.4.

Table 3.5 The properties of Brass-RDE

Property	Value
Disk diameter	10.0 mm
Shroud diameter	25.0 mm
Tip shroud length	25.0 mm
Maximum immersion	12.0 mm
Maximum rotation rate	1500 rpm
Temperature range	10 – 80^{o}C

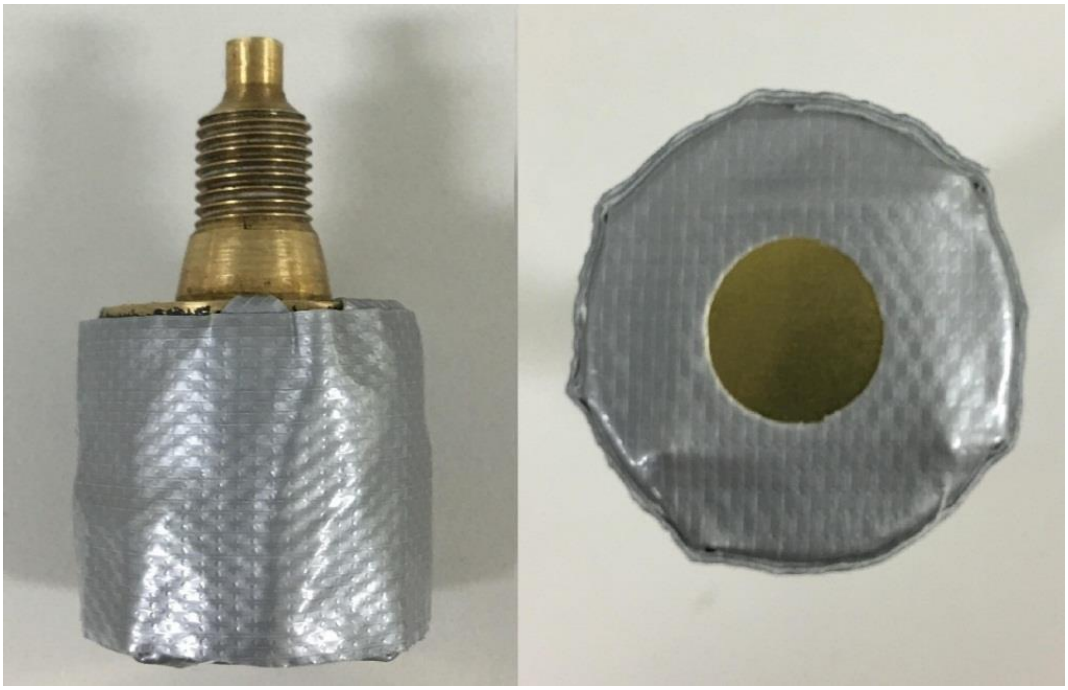

Figure 3.4 The image of Brass-RDE

Nickel rod was used as counter electrode in order to keep Ni ion concentration of electrolyte constant. It was purchased from Alfa Aesar at solid state. Table 3.6 gives the properties of nickel.

Table 3.6 The properties of Ni

Property	Value
Purity	99.5 %
Length	14 cm
Diameter	0.5 cm

The double junction Ag/AgCl (saturated KCl) reference electrode which was preferred for minimizing filling solution contamination of the test electrolyte was ordered from Pine Research Instrumentation. Table 3.7 gives the properties of double junction Ag/AgCl (saturated KCl) reference electrode. Figure 3.5 shows double junction Ag/AgCl (saturated KCl) reference electrode.

Table 3.7 The properties of double junction Ag/AgCl (saturated KCl) reference electrode [52]

Property	Value
Standard potential	-199 mV vs. normal hydrogen potential
Filling solution	4 M KCl
Temperature range	10 – 80^{o}C
Typical variance	±3 – 5 mV

Figure 3.5 The image of double junction Ag/AgCl (saturated KCl) reference electrode

3.2. Electrodeposition of Ni/TiC Nanocomposites

For the production of Ni/TiC nanocomposites, the procedure of Ni/TiC electrodeposition whose schematic is given in Figure 3.6 is followed.

Watts solution, which is an aqueous solution of $NiSO_4.6H_2O$, $NiCl_2.6H_2O$ and H_3BO_3, containing TiC and different concentration of PEI was used as the electrolyte. Chemical composition of Watts bath is shown in Table 3.8. The pH of Watts solution was adjusted to 4.4 at room temperature by the addition of 1 M NaOH.

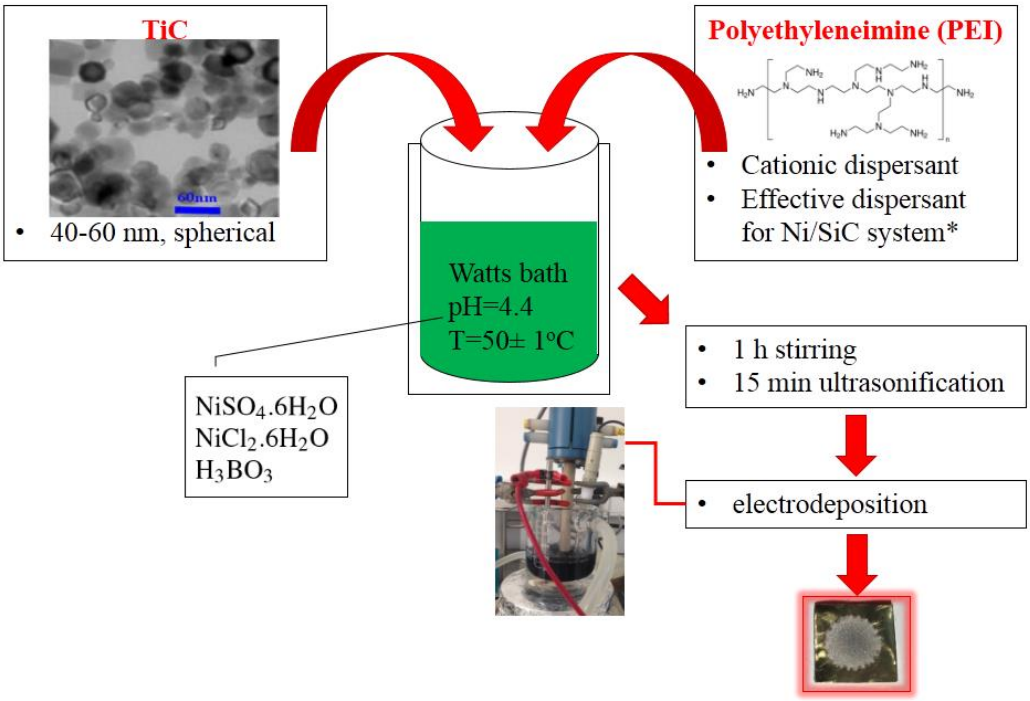

Figure 3.6 Schematic of Ni/TiC electrodeposition procedure

Table 3.8 The composition of Watts solution

Compounds	**Composition (g L^{-1})**
$NiSO_4.6H_2O$	300
$NiCl_2.6H_2O$	35
H_3BO_3	40

In order to keep the temperature constant at 50°C, a jacketed beaker with a water circulating bath was used. First, Watts solution was added to the jacketed beaker. Then, TiC nanoparticles at desired concentration (5 g L^{-1}, 10 g L^{-1} and 20 g L^{-1}) and PEI at desired concentration (0 ppm, 50 ppm, 100 ppm, 125 ppm, 150 ppm,

200 ppm and 250 ppm) were added to the jacketed beaker. The solution was stirred at 500 rpm for 1 hour. Then, the solution was sonicated for 15 minutes in order to prevent the agglomeration of TiC particles. Biopotentiostat (Pine Instrument Company) combined with MSRX Speed Control (Pine Instrument Company) was used for the electrodeposition of Ni/TiC nanocomposites. As the working electrode, a portable Brass-RDE was designed. Figure 3.7 shows the preparation of the Brass-RDE. Ni rod was used as the counter electrode and Ag/AgCl (saturated KCl) electrode was used as the reference electrode. Three electrodes were immersed in the Watts bath.

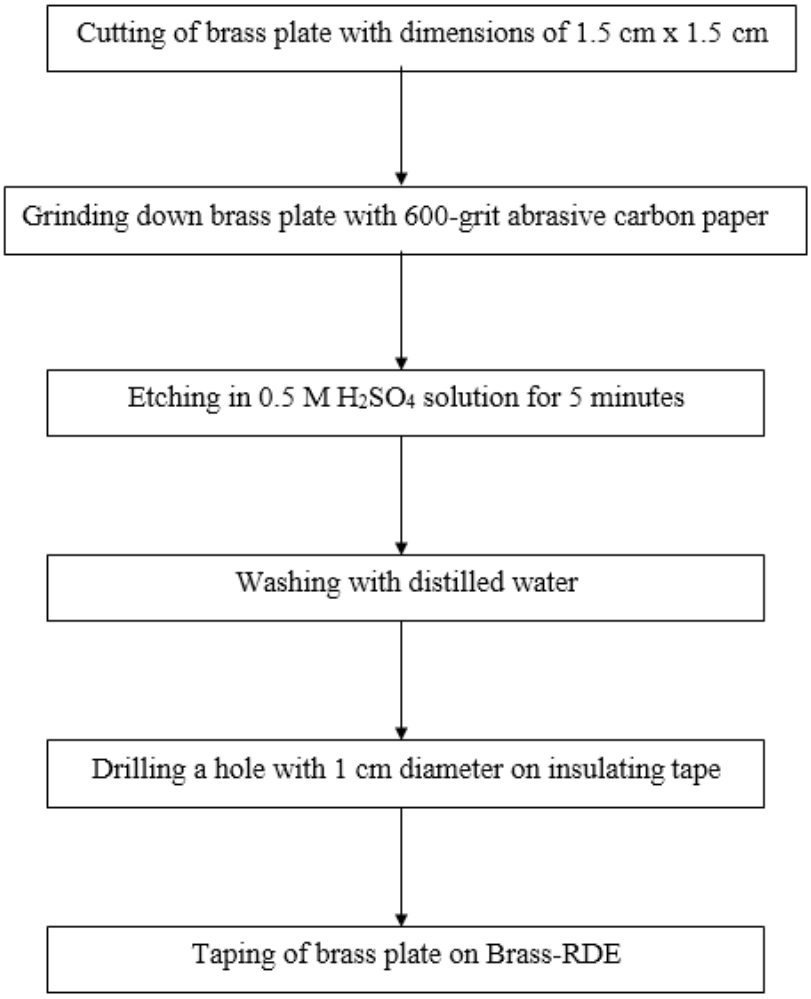

Figure 3.7 The preparation of Brass-RDE

Before each experiment, Ni film with a thickness of ~10 nm was deposited on the cathode with a current density of -10 mA cm^{-2} for 30 seconds as a pretreatment. Then, three electrodes were immersed in a Watts bath containing different concentrations of TiC and PEI for the electrodeposition of Ni/TiC. The electrolyte was also magnetically stirred at a rate of 300 rpm during the electrodeposition. The setup is shown in Figure 3.8.

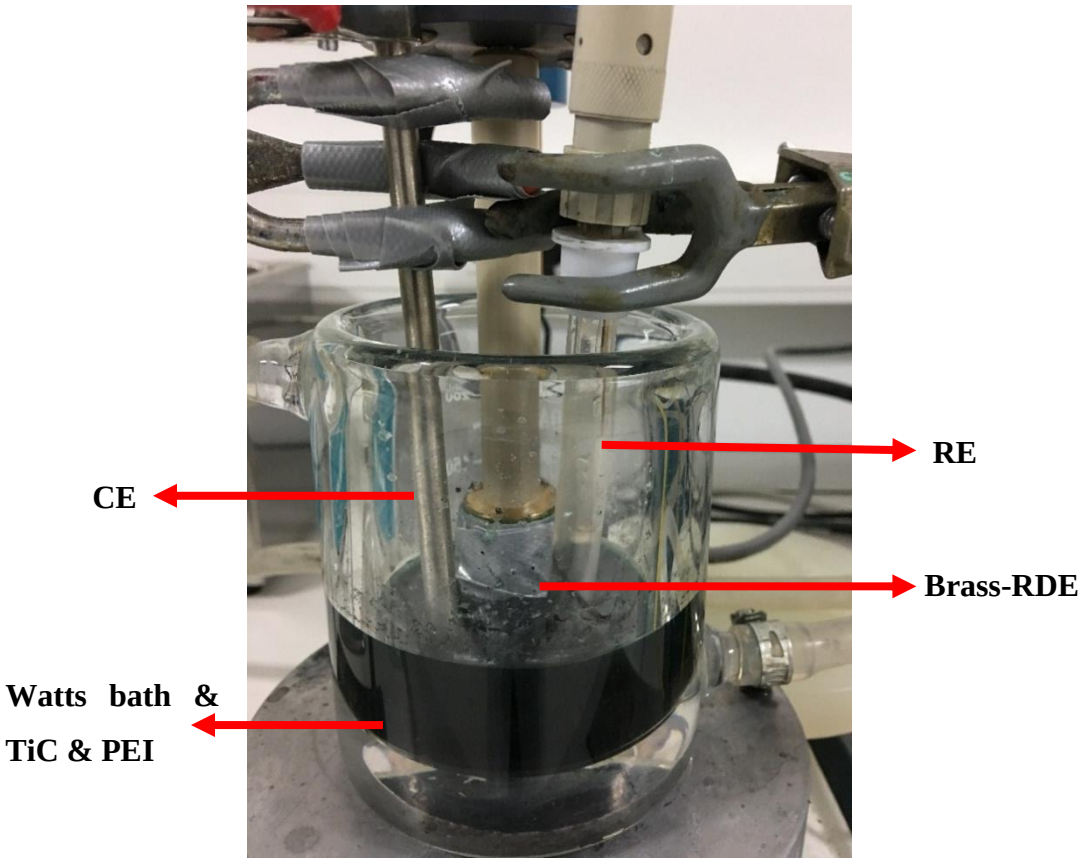

Figure 3.8 Three electrodes in the electrolyte

In order to investigate the effect of critical parameters on Ni/TiC electrodeposition, the different electrodeposition conditions were performed by using galvanostatic

mode of the biopotentiostat under DC. Table 3.9 and Figure 3.9 gives the electrodeposition conditions and setup, respectively.

Table 3.9 The electrodeposition parameters

Property	Value
TiC electrolyte concentration	0, 5, 10 and 20 g L^{-1}
PEI electrolyte concentration	0, 50,100, 125,150 and 200 ppm
Current density for electrodeposition	-10, -25, -50 and -100 mA cm^{-2}
Rotation speed	100, 400 and 900 rpm

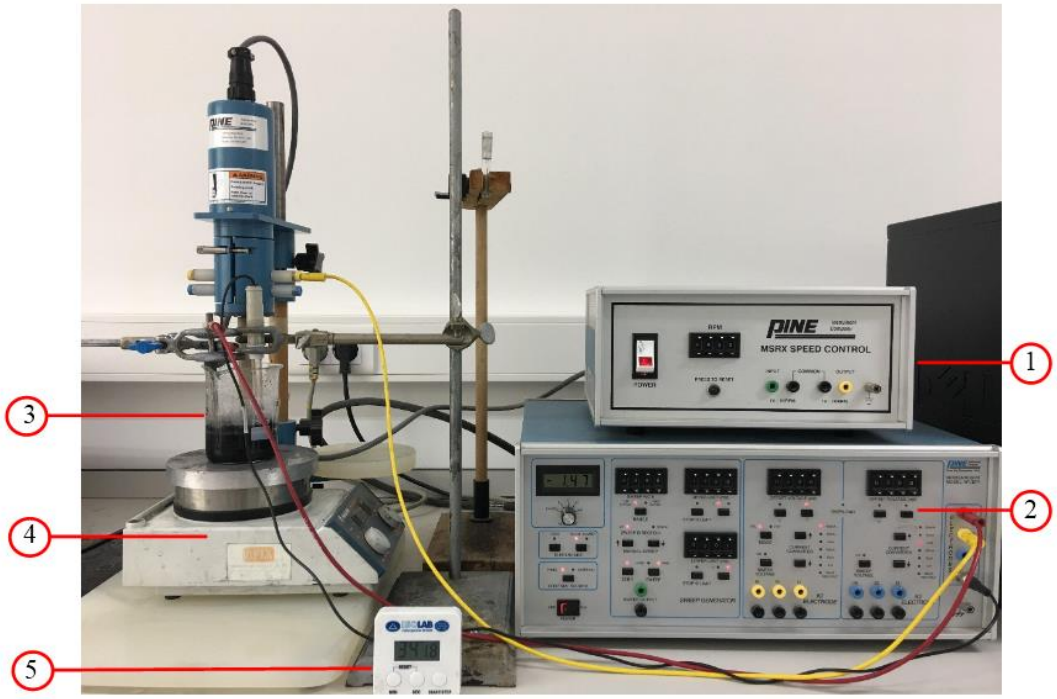

Figure 3.9 The electrodeposition setup

where;

1: RDE rotation speed controller

2: Biopotentiostat

3: Three electrode system

4: Magnetic stirrer

5: Chronometer

Three replicate nanocomposite films for each parameter were produced with a thickness of ~10 μm for SEM/EDS analysis or 20 μm for hardness measurements. The thickness of the deposit can be estimated by Faraday's Law.

3.3. Characterization of Ni/TiC Electrodeposition

Characterization of Ni/TiC electrodeposition can be divided into four main titles. These are the characterization of the dispersion of TiC nanoparticles, characterization of the Ni/TiC electrodeposition kinetics, characterization of the TiC amount in the deposit and characterization of the nanocomposite in terms of morphological and mechanical properties.

3.3.1. Characterization of Dispersion of TiC

In order to characterize the dispersion of TiC in the electrolyte, zeta potential analysis is used. Zeta potential analysis is a technique for determining the surface charge of nanoparticles in the solution. Figure 3.10 shows the electrical double layer at the surface of solution-phase nanoparticle.

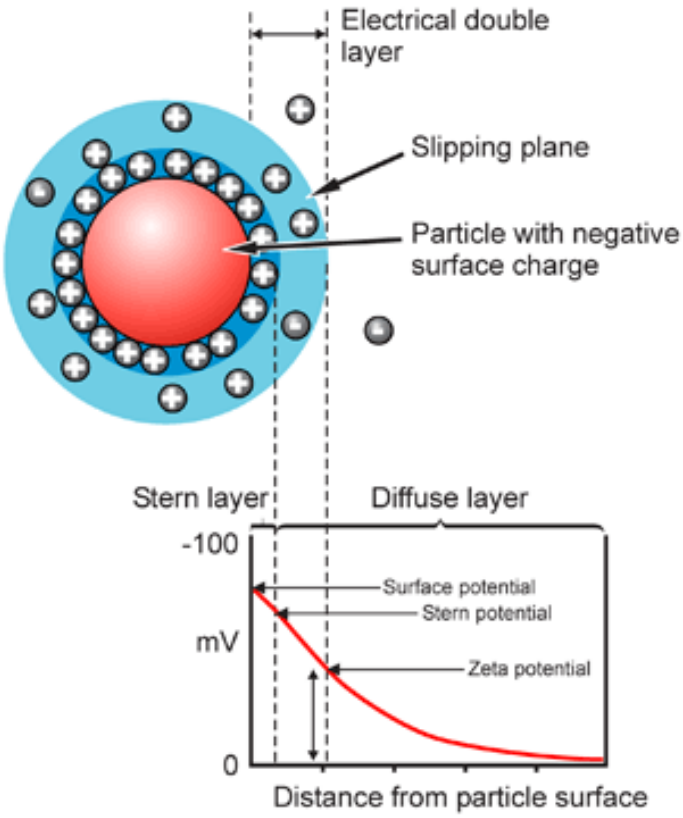

Figure 3.10 The electrical double layer [53]

The zeta potential analysis plays a key role for determination of the stability of TiC particles in the electrolyte. The relationship between the zeta potential and the stability behavior of the colloid as shown in Table 3.10. According to Table 3.10, increasing absolute value of zeta potential results in increasing stability of the colloidal system.

Table 3.10 The relation between the zeta potential and particle stability [54]

Zeta potential (mV)	**Stability behavior of the colloid**
0 to ± 30	Unstable
≥ +30 or ≤ -30	Stable

Before the production of the Ni/TiC nanocomposites, in order to characterize the effect of the dispersant electrolyte concentration on the dispersion of TiC nanoparticles in the electrolyte, the stability of the TiC nanoparticles was investigated by measuring the zeta potential of TiC particles.

Since Watts solution has high ionic conductivity, it is not possible to measure TiC nanoparticle stability in a Watts bath. Therefore, zeta potential measurements were performed for TiC in 0.01 M NaCl solution [40]. Different PEI electrolyte concentration: TiC electrolyte concentration (ppm:ppm) samples were prepared. Table 3.11 gives the zeta potential analysis parameters.

Table 3.11 The zeta potential analysis parameters

Property	**Value**
PEI electrolyte concentration: TiC electrolyte concentration	0, 0.010, 0.025 and 0.050 ppm:ppm
pH	4.4
Temperature	25^{o}C

Dilution solution should have same pH, ionic concentration and polymer concentration with the corresponding sample for correct zeta potential measurement. Thus, dilution samples were prepared by imitating the corresponding sample. The only difference between the sample and dilution solution was dilution solution does not contain TiC particles. The schematic of the preparation of samples for zeta potential analysis are shown in Figure 3.11. The zeta potential measurements were performed by using MALVERN Nano ZS90.

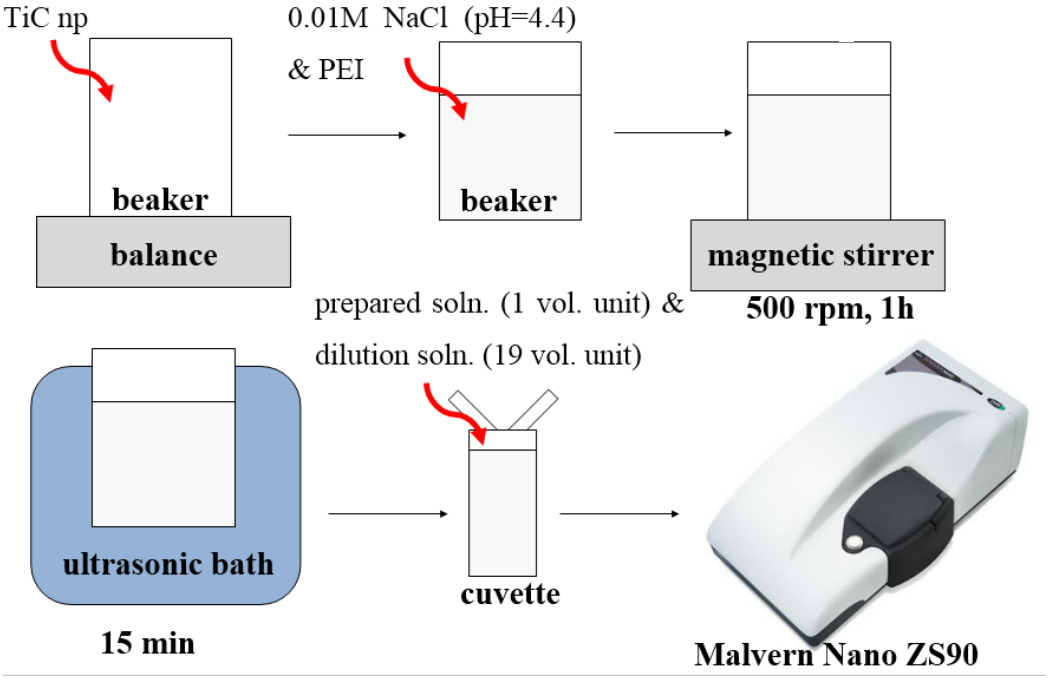

Figure 3.11 The preparation of samples for zeta potential analysis

3.3.2. Characterization of Ni/TiC Electrodeposition Kinetics

Using a dispersant (PEI) improves the stability of TiC particles in the electrolyte. Thus, the distribution of ceramic particles in Ni matrix becomes more uniform. In addition, the affinity of TiC towards the cathode might be enhanced [40]. However, using a dispersant affects the electrodeposition kinetics negatively by occupying the active sites of electrode for nickel electrodeposition. Therefore, it is important to characterize Ni/TiC electrodeposition kinetics. For this purpose, LSV technique and current efficiency measurements were used.

LSV is a technique that measures the current at the working electrode (RDE) while the potential between the working electrode and the reference electrode is varied linearly in time. The output of LSV technique is current vs. potential relation. It is important to determine the initial and final potentials for LSV. In addition, sweep

rate should be determined carefully. By using LSV, the effect of PEI electrolyte concentration on the overpotential was investigated.

LSV analysis and current efficiency measurements were performed by using Biopotentiostat (Pine Instrument Company) combined with MSRX Speed Control. As the working electrode, Pt-RDE was preferred. Ni rod was used as the counter electrode in order to keep Ni ion concentration in the electrolyte constant. As the reference electrode, Ag/AgCl (saturated KCl) reference electrode was used.

Before LSV, Pt-RDE electrode was cleaned electrochemically in 0.5 M H_2SO_4 solution by 100 cycles of cyclic voltammetry between 1.7 V and -0.3 V. After that, by using pure Watts solution nickel was deposited on the cathode for 30 seconds with a current density of -10 mA cm^{-2} as a pretreatment. Then, electrodeposition setup which is shown in Figure 3.12 was prepared. The experimental parameters for LSV are given in Table 3.12. After LSV analysis, deposited film was stripped in 0.2 M HCl solution by applying a current density of 50 mA cm^{-2}.

For current efficiency measurement, first nickel was deposited on the cathode for 30 seconds with a current density of -10 mA cm^{-2} as a pretreatment by using pure Watts solution. After that, co-deposition of Ni/TiC on Pt-RDE was performed in a Watts bath containing TiC nanoparticles and different PEI concentrations with a current density of -50 mA cm^{-2} for 10 minutes. Then, electrodeposited film was stripped in 0.2 M HCl solution with a current density of 50 mA cm^{-2} by monitoring potential. When deposit was completely stripped, the potential suddenly increased. The time for stripping of deposited film was recorded and the current efficiencies were calculated using the Faraday's Law. The parameters for current efficiency measurement are given in Table 3.13.

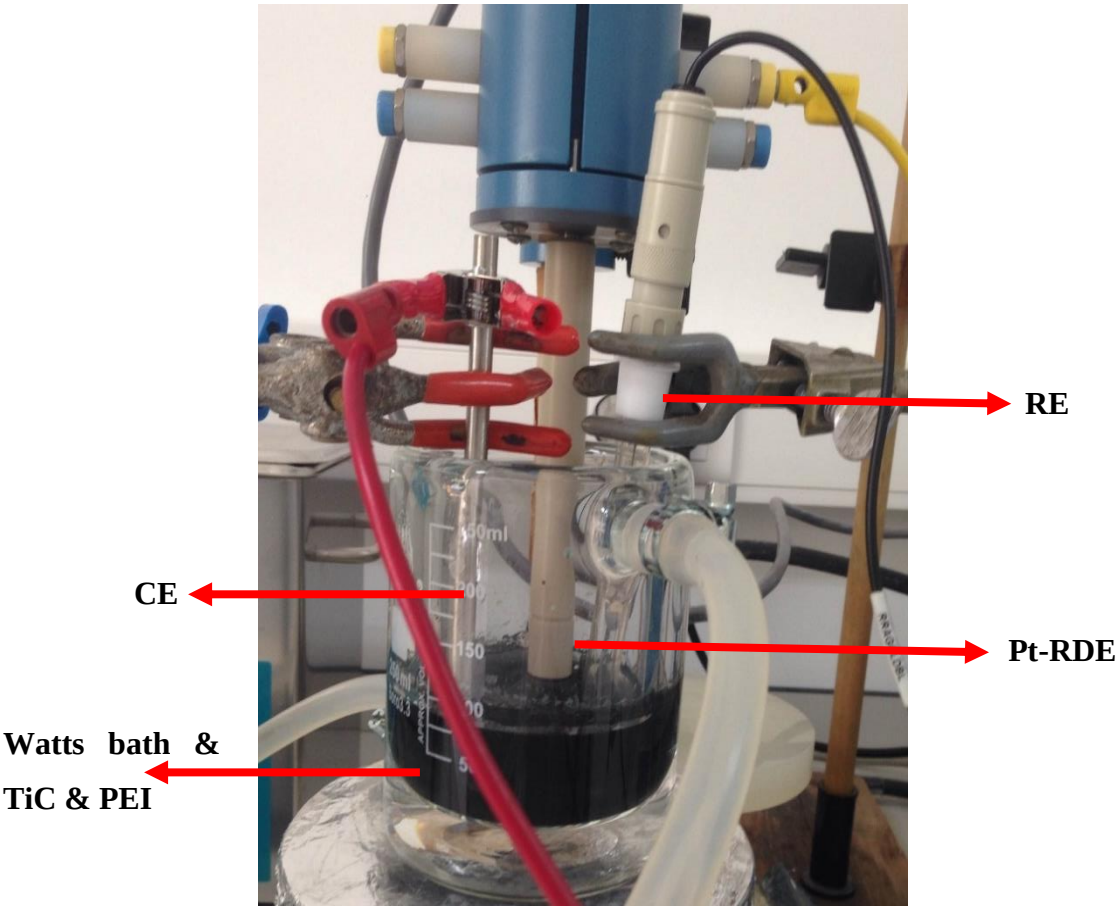

Figure 3.12 LSV and current efficiency measurements setup

Table 3.12 The LSV parameters

Property	Value
TiC electrolyte concentration	0, 5 g L^{-1}
PEI electrolyte concentration	0, 50, 125, 250 ppm
Sweep potential limits	-0.6 V to -1.2 V
Sweep rate	5 mV s^{-1}
Rotation speed	2500 rpm

Table 3.13 The current efficiency measurement parameters

Property	Value
TiC electrolyte concentration	5 g L^{-1}
PEI electrolyte concentration	0, 50, 125, 200 and 250 ppm
Current density for electrodeposition	-50 mA cm^{-2}
Current density for stripping	50 mA cm^{-2}
Rotation speed	400 rpm

The current efficiency was calculated by using equation 3.1.

$$Current\ efficiency\ (\%) = \frac{i_{Ni\ electrodeposition}}{i_{total}} \times 100 \qquad \text{Equation 3.1}$$

Current efficiency is the percentage of the electrochemical equivalent current density for a specific reaction to the total applied current density. According to the Faraday's Law, total amount of chemical change is directly proportional to the quantity of electricity passing [55]. Equation 3.2 shows the Faraday's Law.

$$m = \frac{M \times Q}{N \times F} \qquad \text{Equation 3.2}$$

However, in the nickel electrodeposition some of the applied current is used for hydrogen evolution reaction at the cathode, since nickel reduction and hydrogen evolution reactions have similar reaction potential. These reactions are given in Equation 3.3 and Equation 3.4 at a pH of 4.4 [4].

$$Ni^{2+} + 2e^{-} \rightarrow Ni \qquad U = -0.46\ V\ vs.Ag/AgCl \qquad \text{Equation 3.3}$$

$$2H^{+} + 2e^{-} \rightarrow H_2 \qquad U = -0.49\ V\ vs.Ag/AgCl \qquad \text{Equation 3.4}$$

Therefore, current efficiency basically gives the percentage of the applied current that is used for nickel electrodeposition. Thus, it is a significant indicator in the determination of the electrodeposition kinetics.

3.3.3. Characterization of the TiC Amount in the Deposit

The amount of the reinforcement material in the composite is one of the most crucial parameter for the characterization of these composites. In order to determine the amount of the ceramic particle in the deposit, scanning electron microscopy (SEM) and energy dispersive x-ray spectroscopy (EDS) analysis are commonly used techniques for Ni/TiC composites [1], [2], [18]–[20], [22], [23]. Thus, SEM was used to investigate the morphology and TiC distribution. Moreover, EDS was used to determine the TiC amount in the deposit quantitatively. For this purpose, QUANTA 400F Field Emission Scanning Electron Microscope with EDS was utilized. SEM images were obtained with Everhart-Thornley Detector (ETD) or Back-scattered Electron Detector (BSED). BSED was used to detect Ni and Ti, which exists due to TiC, by using their atomic mass differences. Two constituents can be differentiated based on the contrast. As a result, element of lower atomic mass, which is Ti in this case, appears darker than Ni [56]. Both SEM and EDS analysis were performed under high vacuum and accelerating voltage of 20.0 kV. For EDS analysis, three parallel samples were produced. For each replicate, five different regions of the nanocomposite which are center, top-right, top-left, bottom-left and bottom right were analyzed. The instrument gave the result in terms of Ti weight percentage. By using Equation 3.5, results were converted to TiC volume percentage. Sample calculations for TiC vol.% can be seen in Appendix A.

$$TiC\ vol.\% = \frac{Ti\ wt.\% \times \frac{M_{TiC}}{M_{Ti}} \times \frac{1}{\rho_{TiC}}}{Ti\ wt.\% \times \frac{M_{TiC}}{M_{Ti}} \times \frac{1}{\rho_{TiC}} + (100 - Ti\ wt.\%) \times \frac{1}{\rho_{Ni}}} \qquad \text{Equation 3.5}$$

3.3.4. Characterization of the Deposit in terms of Morphological and Mechanical Properties

After the characterization of the dispersion of TiC nanoparticles, electrodeposition kinetics and TiC amount in the deposit, the optimum dispersant electrolyte concentration, TiC electrolyte concentration, current density and rotation speed were determined. After that, in order to examine the improvement of morphological and mechanical properties of the produced nanocomposites, selected nanocomposites were investigated in terms of their morphological and mechanical properties.

For morphological characterization, SEM and Ti mapping analysis were performed by using QUANTA 400F Field Emission Scanning Electron Microscope.

For mechanical characterization, nanoindentation test was utilized by using CSM Instruments Nano-Micro Combitester. The type of the indenter was Berkovich indenter. The load was selected as 10 mN. The results gave the relationship between load (P) and indentation depth (h). By using Equations 3.6, 3.7 and 3.8, nanoindentation hardness (H_{IT}), stiffness (S) and elastic modulus (E_r) were obtained [57].

$$H_{IT} = \frac{P_{max}}{A_r} \qquad \text{Equation 3.6}$$

$$S = \frac{dP}{dh} \qquad \text{Equation 3.7}$$

$$E_r = \frac{1}{\beta} \times \frac{\sqrt{\pi}}{2} \times \frac{S}{\sqrt{A_p(h_c)}} \qquad \text{Equation 3.8}$$

Nanoindentation tests were performed for pure Ni, 5 g L^{-1} TiC & 125 ppm PEI, @-50 mA cm^{-2} current density and 100 rpm rotation speed and 5 g L^{-1} TiC & 125 ppm PEI, @-25 mA cm^{-2} current density and 900 rpm rotation speed samples at least at 6 different points on the deposit.

CHAPTER 4

RESULTS AND DISCUSSION

In this chapter, results and discussion on the characterization of Ni/TiC electrodeposition in the presence of a cationic dispersant PEI in terms of the particle dispersion, electrodeposition kinetics, TiC amount in the deposit and morphological and mechanical properties of the Ni/TiC nanocomposite are presented.

4.1. Characterization of Dispersion of TiC Nanoparticles in the Electrolyte

The effect of PEI on the dispersion of TiC nanoparticles in the electrolyte is characterized using zeta potential analysis. Since Watts solution has high ionic strength around 2M, the zeta potential measurements of TiC nanoparticles are performed in an aqueous solution of 0.01 M NaCl at 25ºC and pH 4.4 instead. Figure 4.1 shows the zeta potential of TiC nanoparticles with respect to PEI electrolyte concentration. In Figure 4.1, x-axis is presented as the ratio of the PEI electrolyte concentration to the TiC electrolyte concentration. For instance, PEI:TiC ratio of 0.01 corresponds to a suspension with 50 ppm PEI and 5 g L^{-1} TiC.

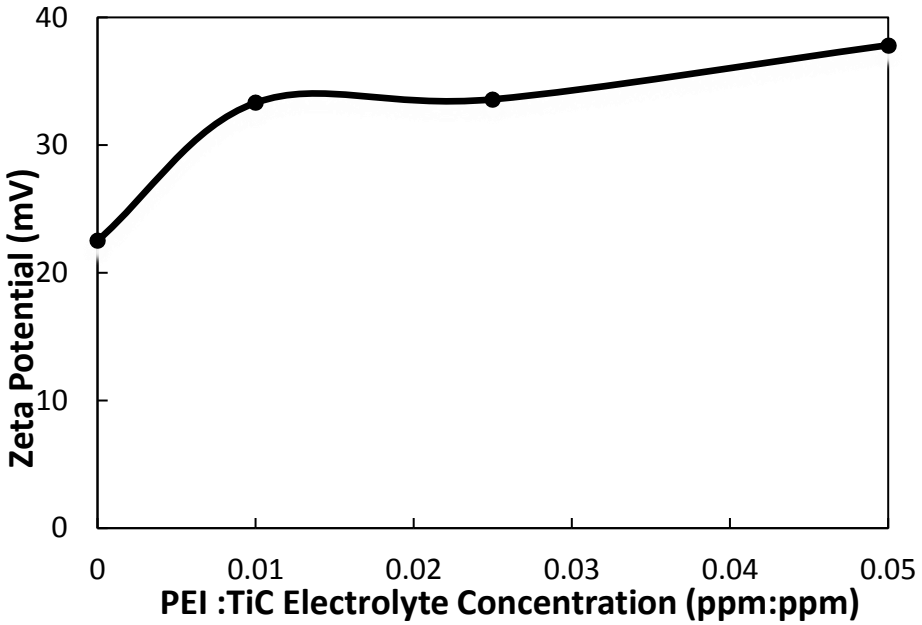

Figure 4.1 Zeta potential of TiC nanoparticles with the addition of PEI at different concentrations in 0.01 M NaCl and at 25°C and pH 4.4

It can be seen in Figure 4.1 that zeta potential of TiC nanoparticles in the absence of PEI is 22.5 mV. The addition of 50 ppm PEI to the suspension increases the zeta potential of TiC nanoparticles sharply to 33.3 mV. The increase in the zeta potential of the particles is less significant after this point; it increases from 33.3 mV to 37.8 mV with the increase of PEI concentration from 50 ppm to 250 ppm. Higher absolute value of the zeta potential means higher repulsive forces between particles. Thus, it may be concluded that the agglomeration of TiC is prevented and stability of the particles in the electrolyte is improved with the addition of PEI even at low concentrations. In the literature, it was stated that the affinity of TiC nanoparticles towards the cathode might be enhanced due to more positively charged TiC nanoparticles [17]. However, the electrostatic effects should not be significant for this case due to the high ionic strength of the Watts bath. To conclude, PEI is highly effective in enhancing the dispersion of TiC nanoparticles and thus particle electrolyte stability even at low concentrations such as 50 ppm.

4.2. Characterization of Electrodeposition Kinetics in the Presence of PEI

As mentioned before, to characterize the electrodeposition of Ni/TiC in terms of the electrodeposition kinetics, linear sweep voltammetry (LSV) and current efficiency measurements were utilized and are discussed in this section.

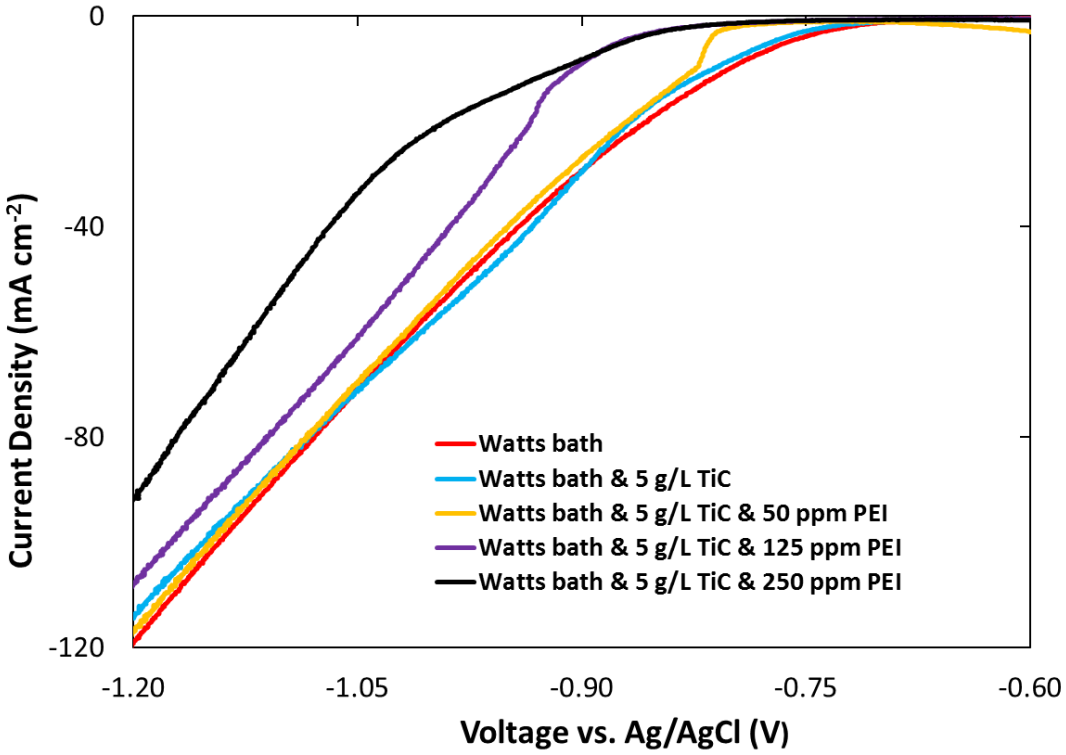

Figure 4.2 Polarization curves for pure Watts solution and Watts solution containing 5 g L^{-1} TiC and different PEI concentrations. The RDE rotation speed is adjusted to 2500 rpm for all cases.

The polarization curves for the Watts solution containing 5 g L^{-1} TiC and different PEI electrolyte concentrations between 0 and 250 ppm are obtained through LSV measurements and shown in Figure 4.2. In Figure 4.2, it can be seen that PEI addition up to 125 ppm cause a slight shift on the polarization curve except at low current densities indicating that nickel electrodeposition is not inhibited

remarkably. On the contrary, significant shift of the polarization curve is observed for the addition of 250 ppm PEI. Therefore, it can be interpreted that nickel electrodeposition is suppressed in the presence of 250 ppm PEI in the electrolyte. This suppression might occur due to the adsorption of polymer onto the electrode. As a result, some of the active sites for charge transfer thus nickel electrodeposition might be blocked. In the literature, there are several explanations for the possible reasons of the inhibition of nickel deposition by the addition of PEI. First one is the ascription of PEI on the electrode surface due to the interactions between the charged imine groups of PEI and nickel ions on the electrode surface [38]. Second reason may be the affinity of PEI towards the electrode surface due to ion-pairing interactions, which results with the blockage of the electrode surface [38].

In order to determine the percentage of the total current used for the nickel electrodeposition, current efficiency measurements are conducted. The average of 3 parallel measurements are presented in Figure 4.3, which gives the current efficiency with respect to the electrolyte concentration of PEI.

According to Figure 4.3, it is seen that, the presence of PEI in the electrolyte does not have a significant effect on the current efficiency up to a concentration of 125 ppm; current efficiency only decreases from 97% to 96.2% with the addition of 125 ppm PEI. However, increasing PEI electrolyte concentration from 125 ppm to 250 ppm results in a significant decrease in the current efficiency from 96.2% to 58.5%. Therefore, in the presence of 250 ppm PEI in the electrolyte, 41.5% of the applied current is used for the hydrogen evolution reaction instead of nickel electrodeposition. Operating at low current efficiencies has two main disadvantages. Firstly, a significant amount of the current is wasted and thus decreases the efficiency of the process. The second one is the absorption of hydrogen into the growing film, which might result in hydrogen embrittlement.

This may lead to reduced ductility and load-bearing capacity of the composite and therefore to crack formations and brittle behavior.

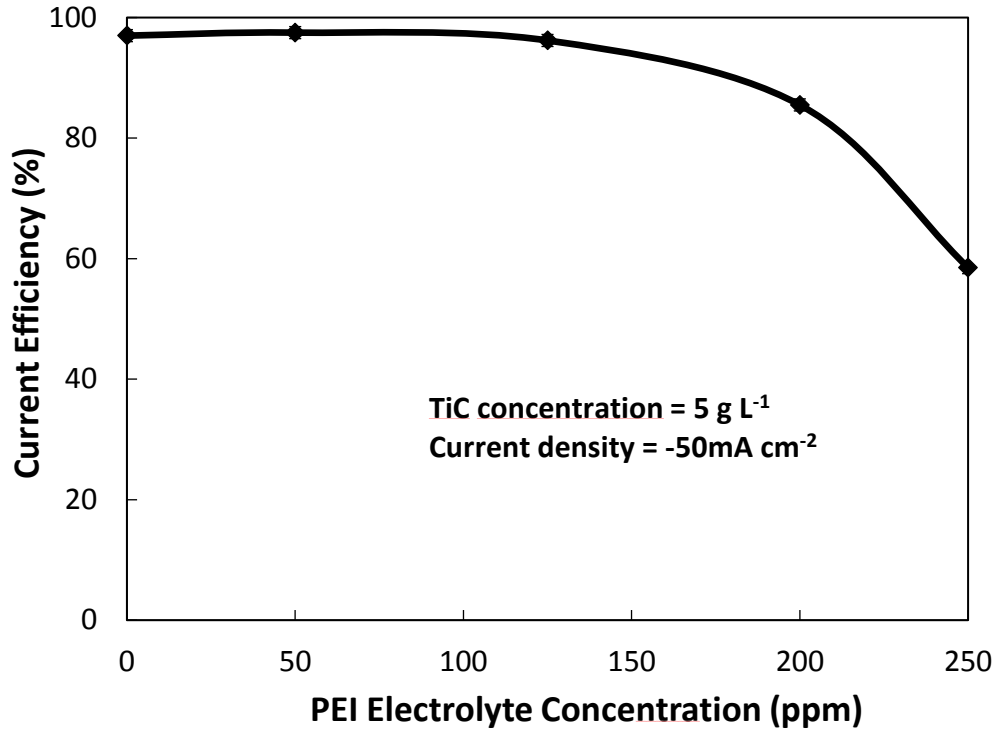

Figure 4.3 The current efficiencies for different PEI concentrations in a Watts bath containing 5 g L^{-1} TiC at a current density of -50 mA cm^{-2}. The RDE rotation speed is adjusted to 2500 rpm for all cases.

It may be concluded that PEI suppresses nickel electrodeposition significantly at electrolyte concentrations of 250 ppm and higher (Figures 4.2 and 4.3). On the other hand, concentrations of PEI up to 200 ppm in the electrolyte enhance the dispersion of TiC particles in the electrolyte without affecting the electrodeposition kinetics remarkably. Because of this observation, upper limit of PEI electrolyte concentration for further studies is determined as 200 ppm, which corresponds to a current efficiency of 85.5%.

4.3. Characterization of TiC Amount in the Deposit

In this part, Ni/TiC nanocomposites are characterized in terms of the TiC amount in the deposit as a function of PEI electrolyte concentration, TiC electrolyte concentration, current density and rotation speed. Three parallel samples of Ni/TiC nanocomposites are produced at an approximate thickness of 10 µm under different conditions in order to investigate the effect of these critical parameters on the TiC incorporation into the deposit. TiC incorporation into the deposit is quantified by measuring the TiC weight percentages in the produced Ni/TiC nanocomposites using SEM/EDS at 5 different points on the same deposit to get an average result for the composite. The typical output of EDS analysis is shown in Figure 4.4.

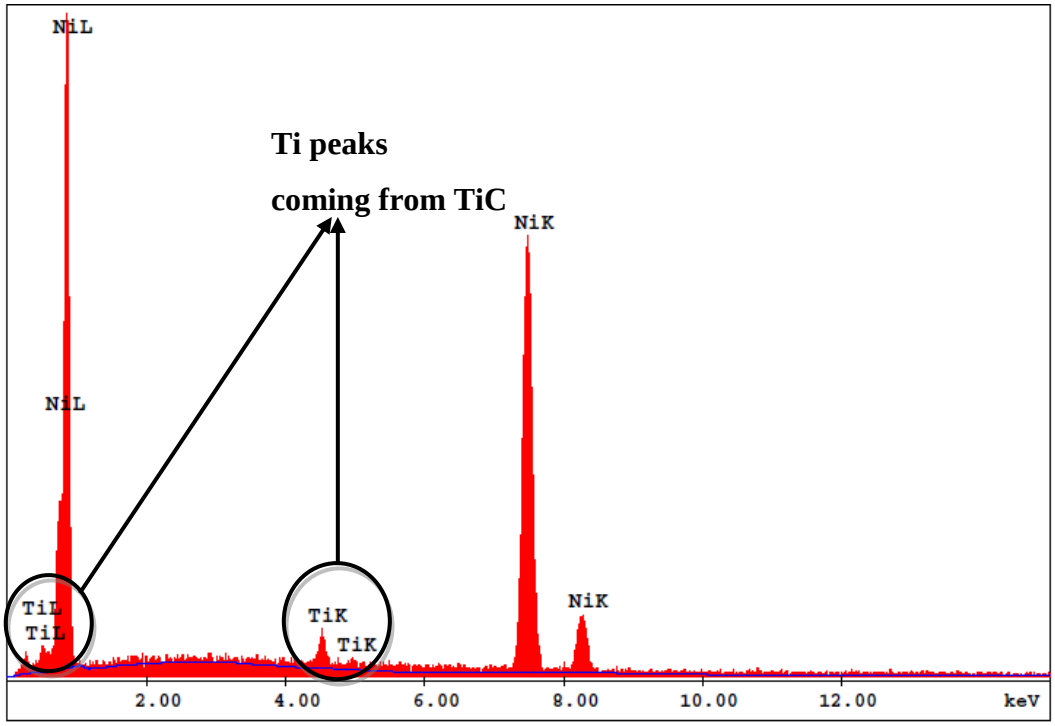

Figure 4.4 EDS result for the Ni/TiC nanocomposite containing 97.88 wt.% Ni and 2.12 wt.% Ti (4.67 vol.% TiC in the deposit)

In the EDS results, titanium peaks are detected due to the TiC content of the Ni/TiC composite. To get an average TiC vol.% in the deposit, first Ti wt.% is converted to TiC vol.%. Then, the average of 5 EDS measurements on the same sample following by the average and standard deviation of 3 parallel samples are calculated. A sample calculation for the TiC vol.% is given in Appendix A. During the EDS analysis, low magnification is preferred in order to be able to cover the largest composite area possible. Using high magnification rates might limit the area analyzed and lead to more localized results. Thus, the average TiC vol.% calculated would be less accurate. To understand the effect of magnification rate on the calculated TiC vol.% Figure 4.5 is given. In Figure 4.5, it is clearly seen that using high magnification gives localized TiC amount on the composite. Therefore, in this study all EDS measurements are conducted at the lowest possible magnification of x200.

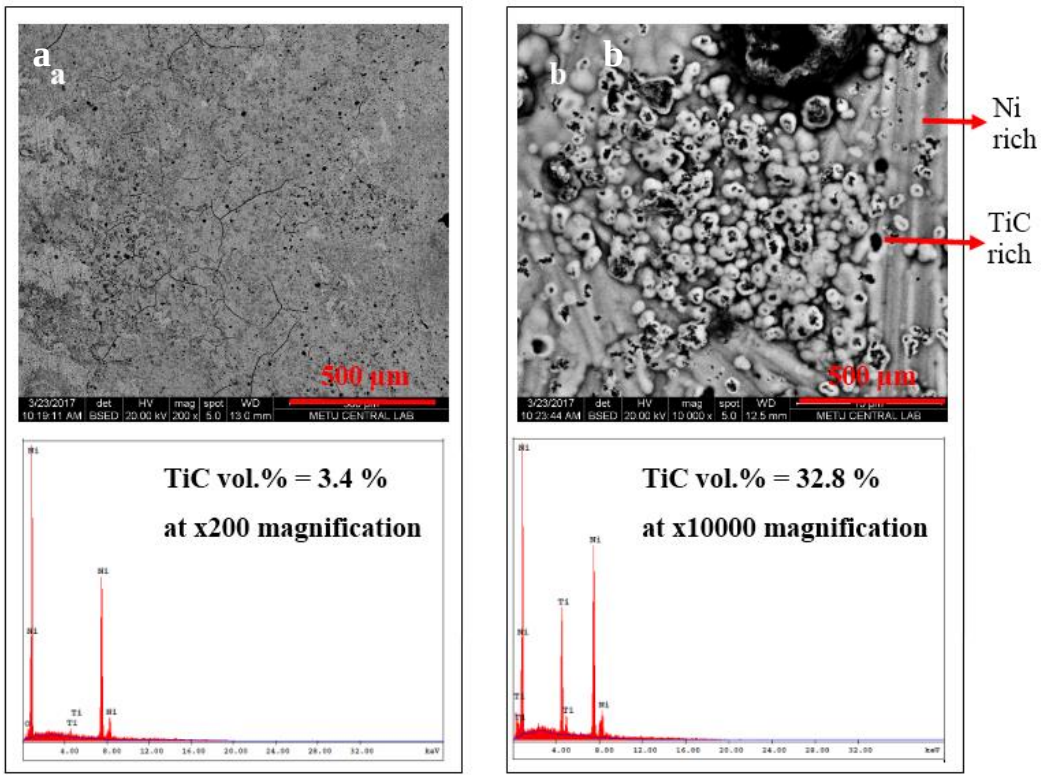

Figure 4.5 SEM micrographs and EDS results for the same nanocomposite at a magnification of a) x200 and b) x10000

4.3.1. Effect of PEI Electrolyte Concentration

In order to characterize the effect of PEI electrolyte concentration on the TiC incorporation, Ni/TiC nanocomposites are produced in a Watts bath containing 5 g L^{-1} TiC and different PEI concentrations of 0 to 200 ppm. TiC amount in the deposit is plotted with respect to PEI electrolyte concentration and shown in Figure 4.6.

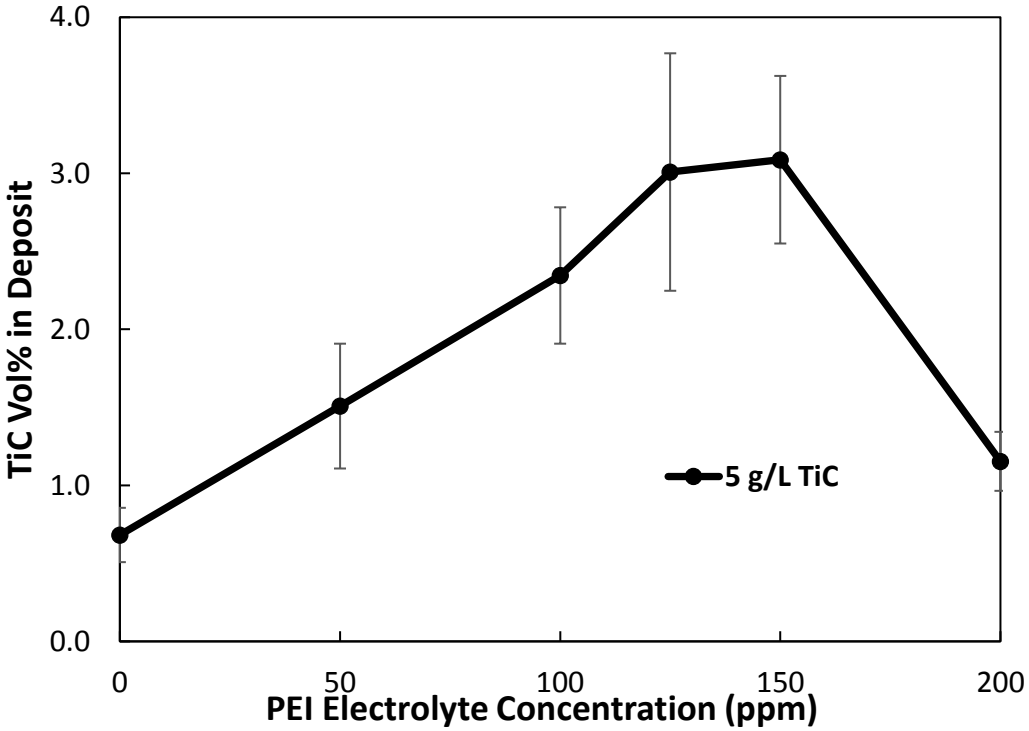

Figure 4.6 TiC vol.% in the deposit for different PEI electrolyte concentrations in a Watts bath containing 5 g L^{-1} TiC at a current density of -50 mA cm^{-2}. The RDE rotation speed is adjusted to 100 rpm for all cases.

It can be seen in Figure 4.6 that increasing PEI electrolyte concentration from 0 to 125 ppm increases TiC vol.% in the deposit from 0.68 vol.% to 3.01 vol.%. This increase in the TiC incorporation might be explained by the improved stability of the TiC particles in the electrolyte at this PEI concentration. A similar trend was also reported for Ni/SiC electrodeposition in the presence of PEI [41]. Figure 4.6

also shows that TiC vol.% remains nearly the same for PEI electrolyte concentrations of 125 and 150 ppm. Further increase in the PEI concentration from 150 ppm to 200 ppm results in a sharp decrease of TiC vol.% in the deposit. To summarize, it can be concluded that 125 ppm PEI addition to a Watts solution containing 5 g L^{-1} TiC results in a considerable increase on the TiC incorporation into the deposit by enhancing the particle dispersion effectively without inhibiting nickel electrodeposition. Therefore, a PEI electrolyte concentration of 125 ppm is used for the rest of the experiments.

Figure 4.7 shows the effect of PEI concentration on the TiC incorporation for a Watts bath containing 10 g L^{-1} and 20 g L^{--1} TiC. To conclude, PEI is an effective dispersant at an electrolyte concentration of 125 ppm and enhances TiC content of the composite for different TiC electrolyte concentrations, especially for 5 g L^{-1} and 10 g L^{-1} TiC in Watts bath.

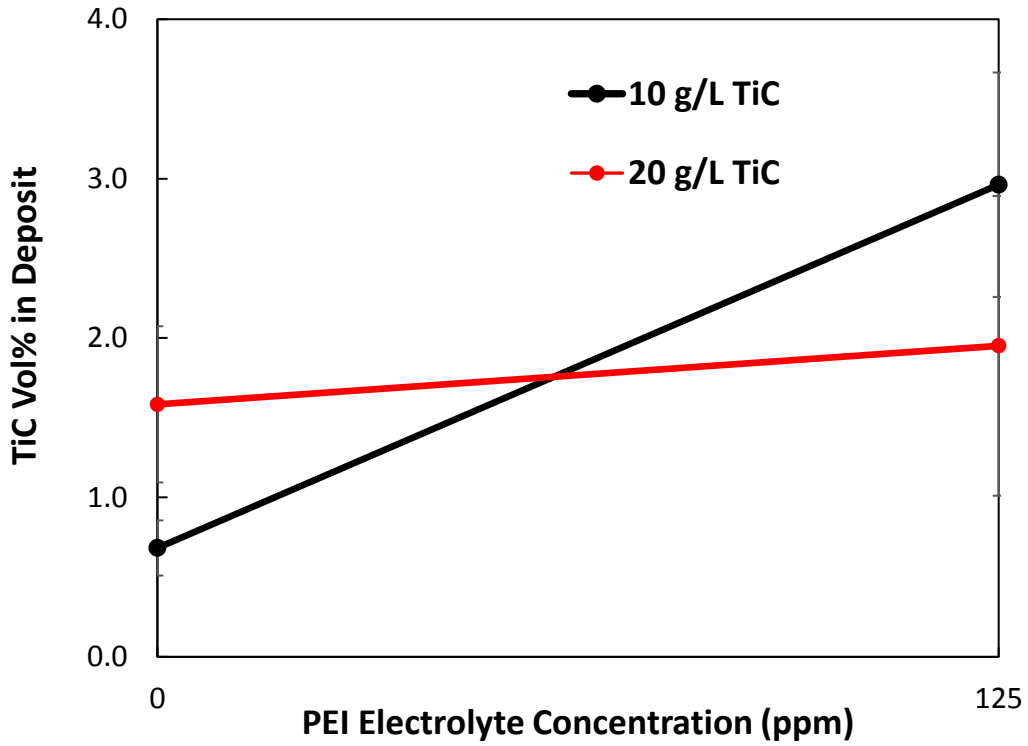

Figure 4.7 TiC vol.% in the deposit for different PEI electrolyte concentrations in a Watts bath containing 10 g L^{-1} and 20 g L^{-1} TiC at a current density of -50 mA cm^{-2}. The rotation speed is adjusted to 100 rpm for all cases.

4.3.2. Effect of Particle Electrolyte Concentration

The effect of particle electrolyte concentration on the TiC incorporation into the deposit is presented in this section. TiC amount in the nanocomposite for different particle electrolyte concentrations from 5 g L^{-1} to 20 g L^{-1} for the addition of 0 and 125 ppm PEI are studied. Figure 4.8 shows TiC vol.% in the deposit with respect to TiC electrolyte concentration.

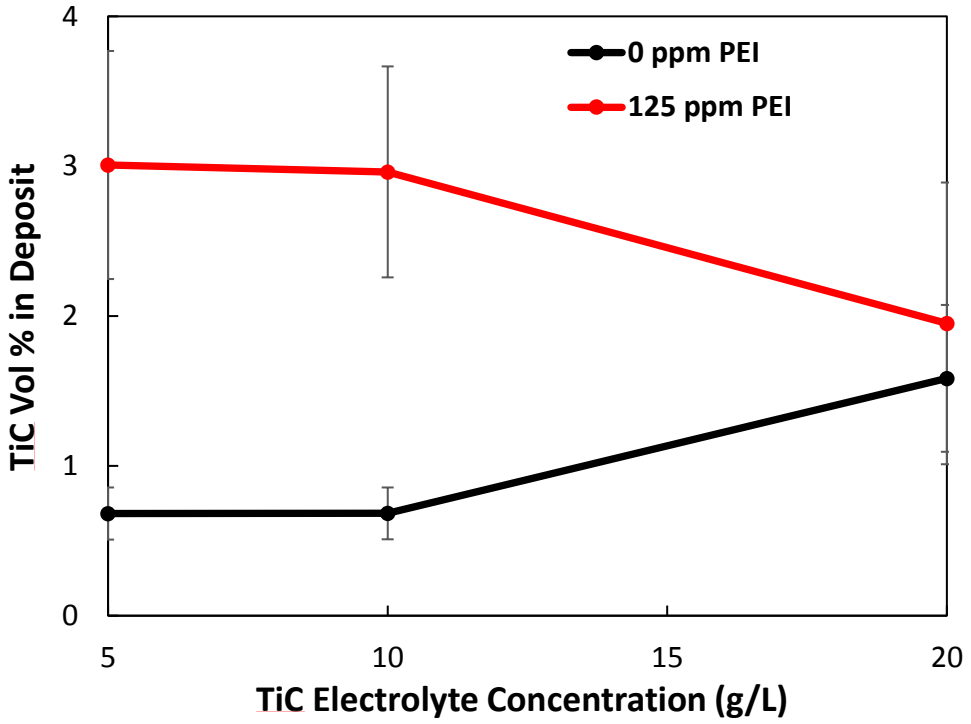

Figure 4.8 TiC vol.% in the deposit for different TiC electrolyte concentrations in a Watts bath containing 0 and 125 ppm PEI at a current density of -50 mA cm^{-2}. The RDE rotation speed is adjusted to 100 rpm for all cases.

In Figure 4.8, it can be seen that increasing TiC electrolyte concentration from 5 g L^{-1} to 20 g L^{-1} does not change TiC vol.% in the deposit significantly. In fact, in the case of 125 ppm PEI addition increasing TiC electrolyte concentration from 5 g L^{-1} to 10 g L^{-1} does not create a major change in the TiC content of the composite. Yet, further increase from 10 g L^{-1} resulted in a decrease in TiC vol.%

in the deposit. In the literature, it has been already stated that particle content in the deposit increases with increasing particle concentration up to certain point and then either remains unchanged [14, 40, 41, 43, 45] or decreases [2, 18]. The trend shown in Figure 4.8 might be similar to the reported descending trends [2, 18]. This decrease in TiC incorporation might occur due to the fact that increasing collisions of particles in the electrolyte decreases the residence time of TiC particles on the electrode surface. In that way, TiC incorporation into the growing composite film might be lowered. The second possible reason of this decrease is that PEI concentration is not enough for high dispersion of TiC so that incorporation of agglomerated TiC into the deposit might become difficult. Thus, incorporation rate of TiC is declined.

To conclude, increasing TiC electrolyte concentration from 5 g L^{-1} to 20 g L^{-1} does not result in a significant increase in the TiC amount in the composite regardless of the PEI present. Moreover, maximum TiC incorporation was achieved as 3 vol.% in Watts bath containing 5 g L^{-1} TiC in the presence of 125 ppm PEI. Therefore, further experiments are done with a Watts bath containing 5 g L^{-1} TiC and 125 ppm PEI in the electrolyte.

4.3.3. Effect of Current Density

In this section, Ni/TiC electrodeposition is characterized as a function of the applied current density. Figure 4.9 shows the TiC vol.% in the deposit with respect to different current densities from -10 mA cm^{-2} to -100 mA cm^{-2} for the electrolyte containing no dispersant or 125 ppm PEI.

According to Figure 4.9, TiC incorporation remains nearly unchanged with respect to the current density in the absence of PEI. It is not possible to come to a conclusion about the dependence of particle incorporation on the current density in the absence of PEI since TiC vol.% in the deposit is smaller than 1% for all current densities. In the case of 125 ppm PEI addition, the current density does not have a

major effect on the particle amount at low current densities. However, further increase of current density leads to a decline of TiC vol.% in the deposit. As it can be seen in Figure 4.9, increasing current density from -25 mA cm^{-2} to -50 mA cm^{-2} results in a decrease of TiC amount in the deposit from 3.91 vol.% to 3.01 vol.%. It is already reported in the literature that at high current densities nickel anions transport to the cathode faster than the TiC particles from the bulk to the cathode and in this way, while nickel deposition is enhanced, TiC incorporation is declined [1]. A similar trend was also observed for Ni/SiC electrodeposition in the presence of PEI [40]. Moreover, a previous model developed for Ni/SiC electrodeposition proposed that increasing current density results with decreasing particle volume fraction in the deposit [14].

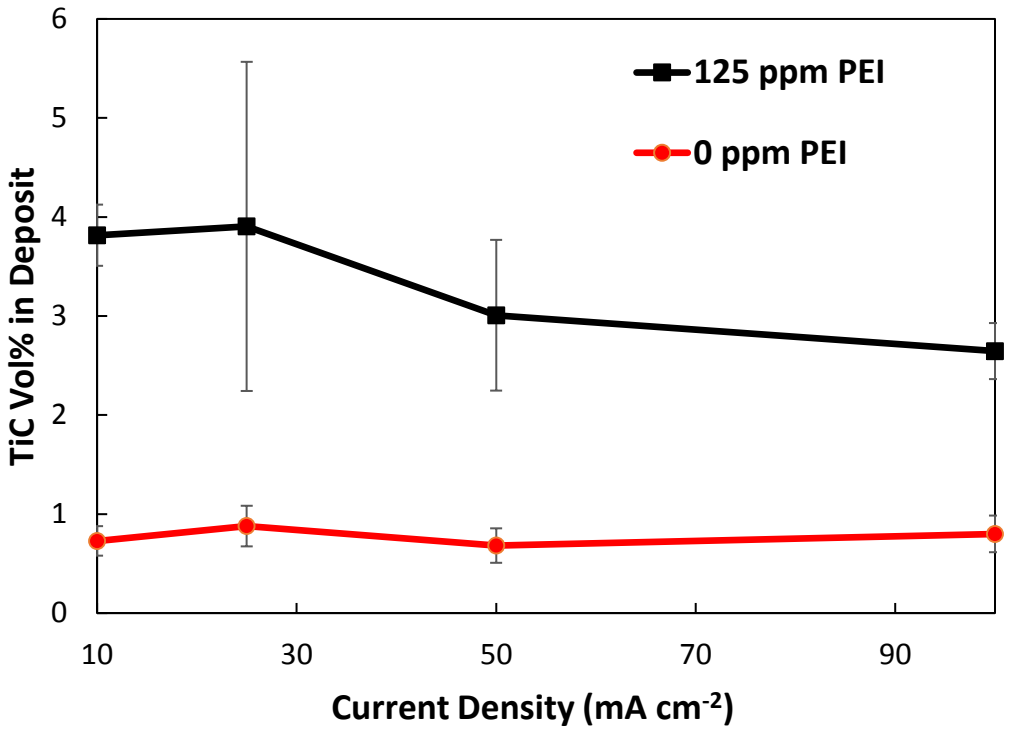

Figure 4.9 TiC vol.% in the deposit for different current densities in a Watts bath containing 5 g L^{-1} TiC in the absence and presence of PEI. The RDE rotation speed is adjusted to 100 rpm for all cases.

The maximum TiC incorporation achieved is 3.91 TiC vol.% in the deposit in the Watts bath containing 5 g L^{-1} TiC and 125 ppm PEI at -25 mA cm^{-2} current density and 100 rpm rotation. However, since the standard deviation for these deposits are much higher indicating that they are less uniform, current density is decided to be kept constant at -50 mA cm^{-2} in the next study.

4.3.4. Effect of Rotation Speed

The hydrodynamic conditions are also very important for the particle incorporation rate since the residence time of a ceramic particle on the cathode surface changes with respect to the rotation speed. Figure 4.10 shows the vol.% in the deposit with respect to different rotation speeds from 100 rpm to 900 rpm.

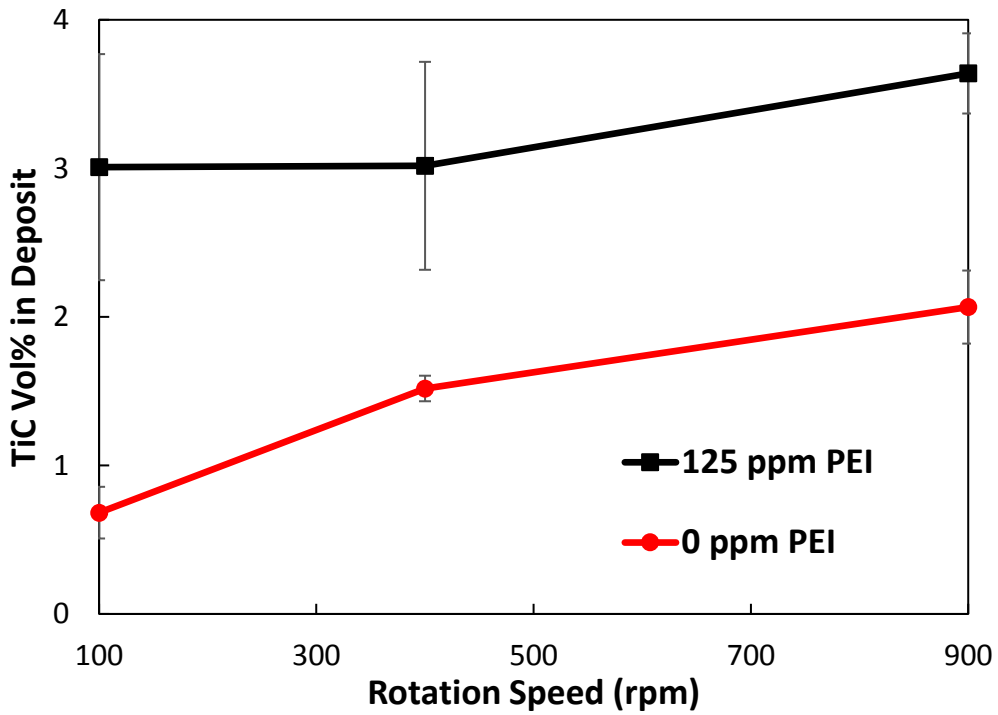

Figure 4.10 TiC vol.% in the deposit for different rotation speeds in a Watts bath containing 5 g L^{-1} TiC in the absence and presence of PEI. The current density is -50 mA cm^{-2} for all cases.

It is seen that increasing the rotation speed of the rotating disk electrode from 100 rpm to 900 rpm increases TiC vol. % in the deposit remarkably for a Watts solution containing no PEI. This increase might be explained by that increasing rotation speed enhances the transport of TiC towards the cathode by convection. In addition, increasing rotation speed increases the residence time of a particle on the cathode surface and enhances the particle incorporation [14]. Yet, very high rotation speeds results in lower particle incorporation rate into the deposit due to increased shear force at the electrode surface [5]. But in this study, such high rotation speeds are not investigated. It can be seen in Figure 4.10 that in the presence of PEI, TiC vol. % in the deposit is a weak function of the rotation speed and increases slightly from 3 vol.% to 3.6 vol.%. Eroglu et al. also observed such a trend for Ni/SiC electrodeposition [40]. It is proposed that the residence time is less sensitive to rotation speed in the presence of the dispersant [14]. As a conclusion, rotation speed increases the TiC incorporation into the deposit. Moreover, it can be concluded that 125 ppm PEI addition to the electrolyte increases TiC content of the composite for all rotation speeds.

4.4. Characterization of Morphological Properties of Nanocomposites

The morphological properties of Ni/TiC nanocomposites are characterized by SEM and Ti mapping experiments and presented in this section. In order to investigate the effect of the dispersant on Ni/TiC nanocomposite surface morphology in terms of the uniformity of TiC particles in the deposit, SEM analysis is used. Figure 4.11 shows the SEM micrographs of the nanocomposites using BSED detector at a magnification of x200.

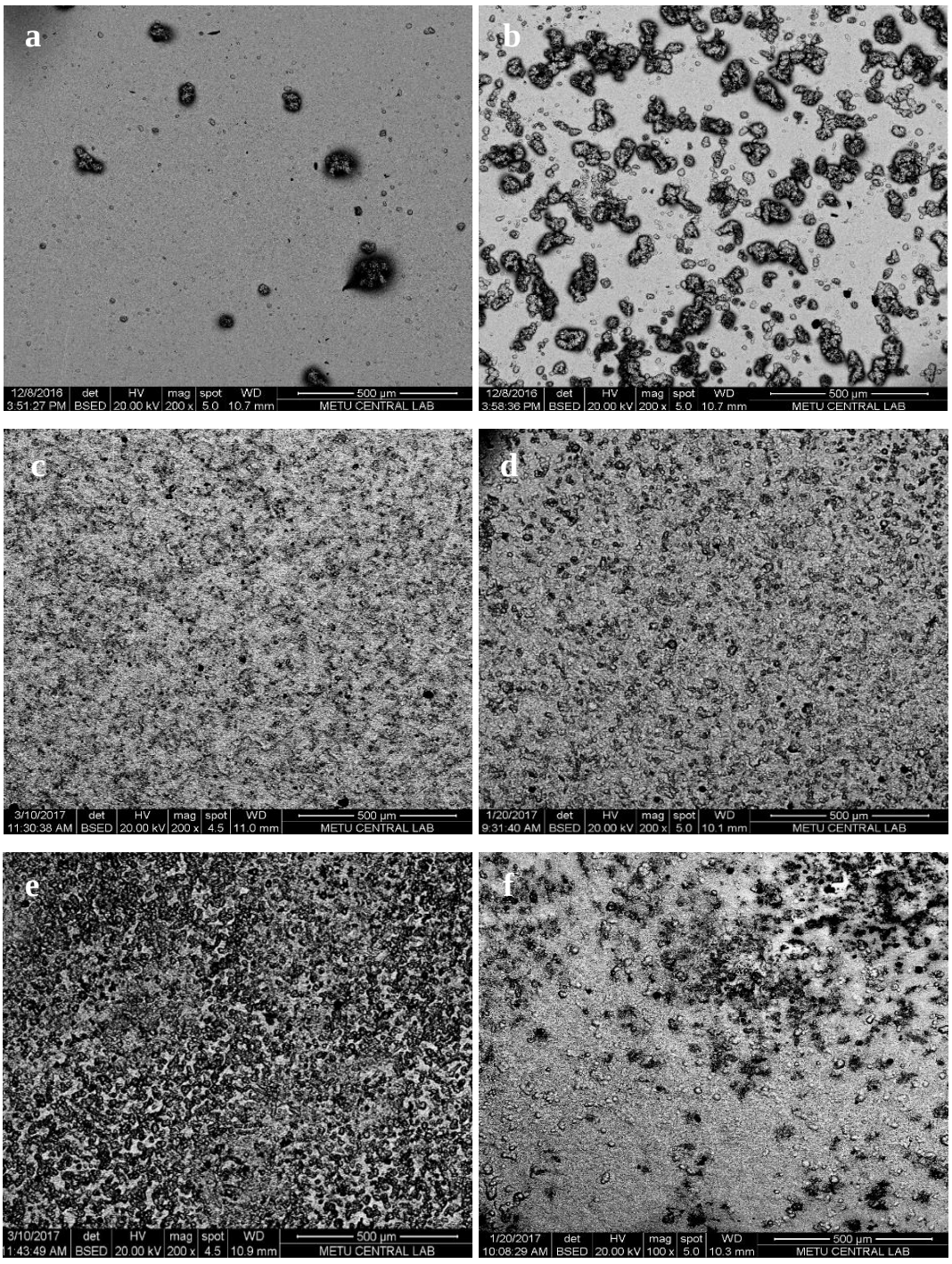

Figure 4.11 SEM micrographs at a magnification of x200 for Ni/TiC nanocomposites produced in a Watts bath containing 5 g L^{-1} TiC and (a) 0 ppm PEI (0.68 vol.% TiC in the deposit), (b) 50 ppm PEI (1.51 vol.% TiC in the deposit), (c) 100 ppm PEI (2.35 vol.% TiC in the deposit), (d) 125 ppm PEI (3.01 vol.% TiC in the deposit), (e) 150 ppm PEI (3.09 vol.% TiC in the deposit), (f) 200 ppm PEI (1.15 vol.% TiC in the deposit). Current density and rotation speed are -50 mA cm^{-2} and 100 rpm for all experiments, respectively.

According to Figure 4.11a, there are some agglomeration of TiC in the nanocomposite obtained in a Watts bath containing 5 g L^{-1} TiC and no PEI. Also, the non-uniform distribution of TiC in the deposit is observed (Figure 4.11a). The addition of PEI up to 150 ppm in Watts bath decreases the agglomeration of TiC in the deposit significantly as apparent in Figure 4.12b-e. In addition, according to Figure 4.11b-e, more uniform and higher incorporation of TiC in the nanocomposite is achieved with increasing PEI electrolyte concentration. Actually, similar TiC distribution without large agglomerates is achieved by using PEI electrolyte concentrations between 100 ppm and 150 ppm. However, non-uniform distribution of TiC in the deposit is detected for nanocomposites produced in a Watts bath containing 5 g L^{-1} and 200 ppm PEI (Figure 4.11f). These results are also in parallel with Figure 4.5. To conclude, it can be said that PEI addition up to 150 ppm decreases the agglomeration of TiC significantly and provides uniformly distributed TiC incorporation into the deposit.

In order to discuss the effect of rotation speed on the morphology of the nanocomposites, the SEM micrographs for the deposit produced in Watts bath containing 5 g L^{-1} TiC and 0 and 125 ppm PEI at a current density of -50 mA cm^{-2} and varying rotation speeds between 100 rpm to 900 rpm are shown in Figure 4.12.

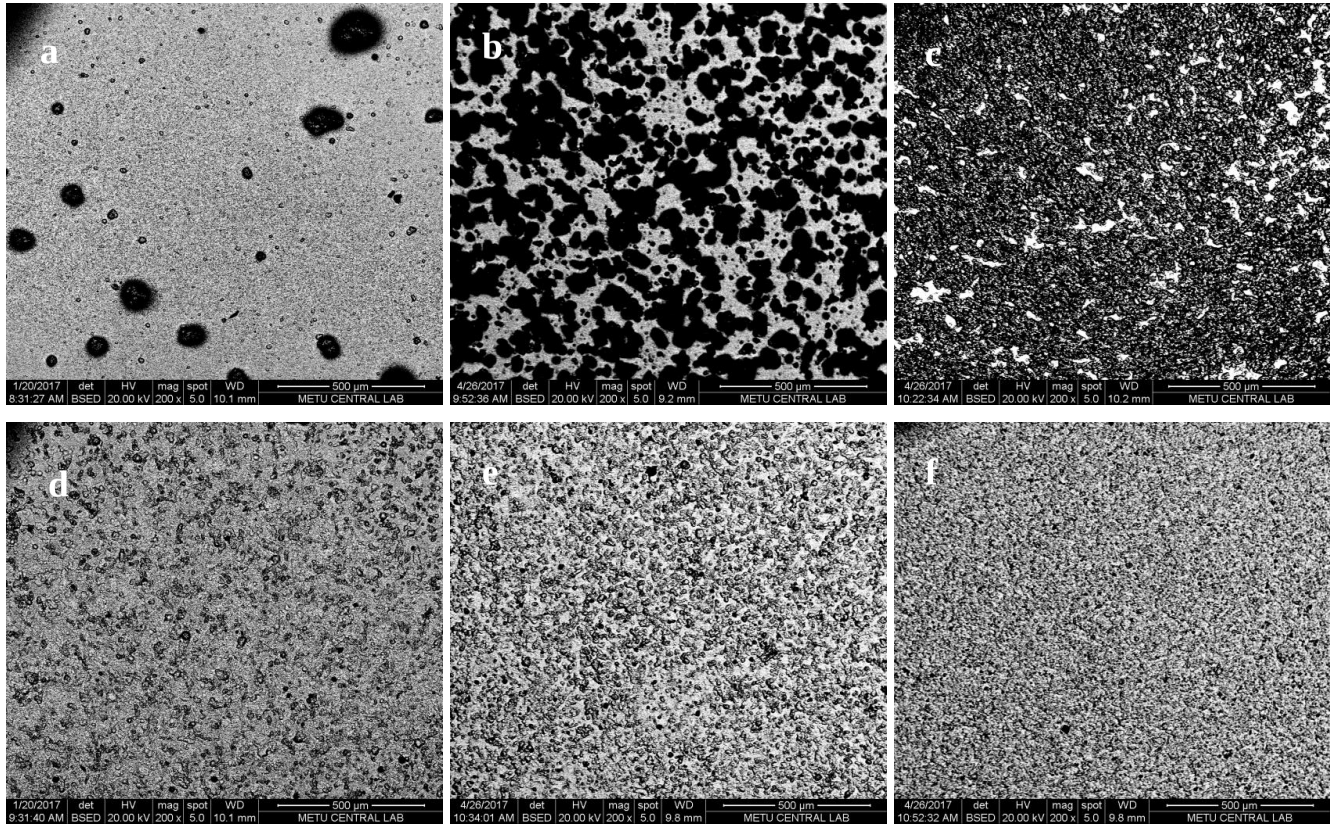

Figure 4.12 SEM micrographs at a magnification of x200 for nanocomposites produced in Watts bath containing 5 g L^{-1} TiC and (a) 0 ppm PEI at 100 rpm (0.68 vol.% TiC in the deposit), (b) 0 ppm PEI at 400 rpm (1.52 vol.% TiC in the deposit), (c) 0 ppm PEI at 900 rpm (2.07 vol.% TiC in the deposit), (d) 125 ppm PEI at 100 rpm (3.01 vol.% TiC in the deposit), (e) 125 ppm at 400 rpm PEI (3.02 vol.% TiC in the deposit), (f) 125 ppm PEI at 900 rpm (3.64 vol.% TiC in the deposit).

In Figure 4.12, it is apparent that increasing rotation speed provides more uniform TiC distribution with smaller agglomerates for the nanocomposites produced in Watts bath without any PEI (Figure 4.12a-c). However, the rotation speed for the case of 125 ppm PEI addition does not have significant impact on the TiC distribution (Figure 4.12d-f). It can be concluded that for all rotation speeds, uniform distribution of TiC in the nanocomposite is achieved in the presence of PEI (Figure 4.12d-f).

In order to compare the morphological properties of produced Ni/TiC nanocomposites with the pure Ni coating, SEM analysis with an ETD detector is utilized. SEM micrographs of pure Ni coating and Ni/TiC nanocomposites produced with and without the addition of PEI into the electrolyte are presented in Figure 4.13.

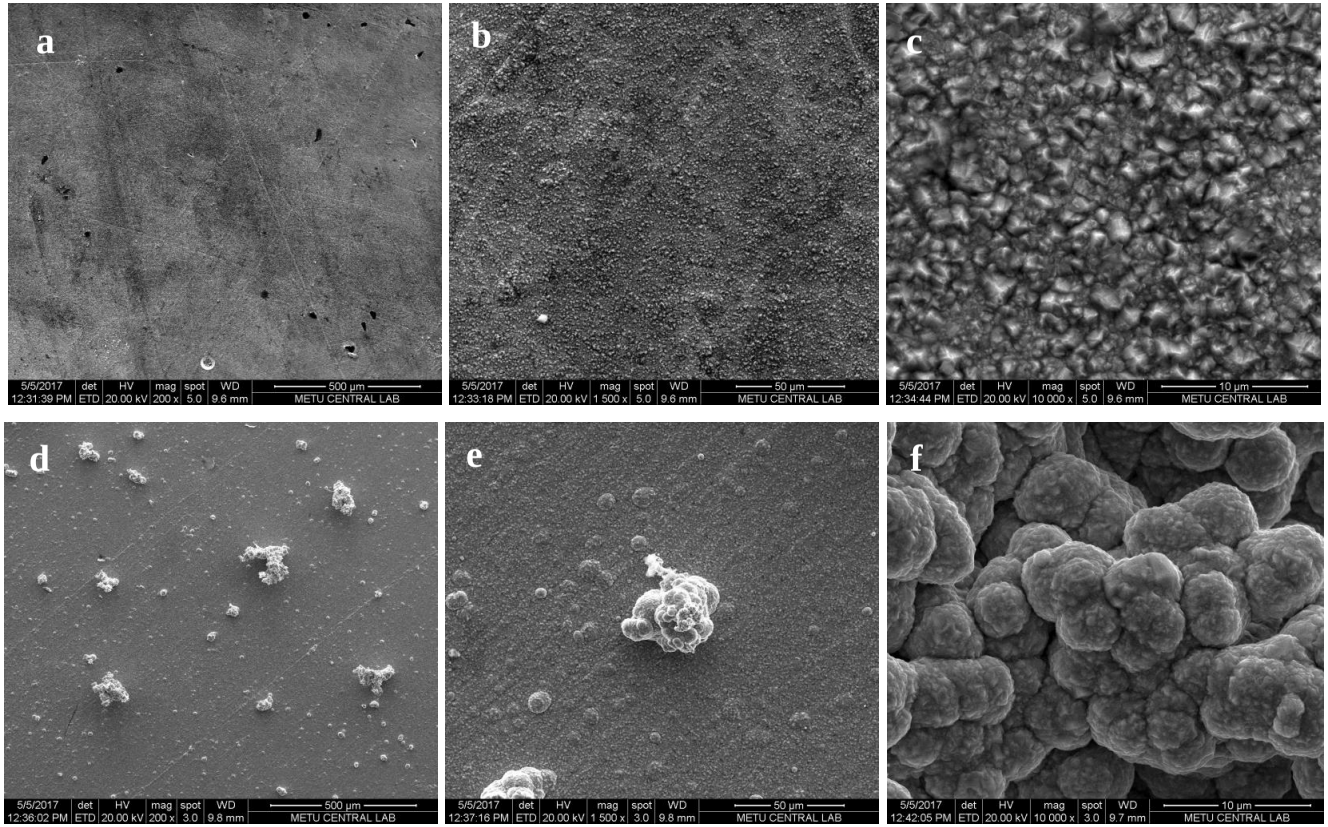

Figure 4.13 SEM micrographs for pure nickel deposit at a magnification of (a) x200, (b) x1500, (c) x10000, Ni/TiC nanocomposite produced in a Watts bath containing 5 g L^{-1} TiC and no PEI at a magnification of (d) x200, (e) x1500, (f) x10000. Current density and rotation speed are -50mA cm^{-2} and 100 rpm for all experiments, respectively.

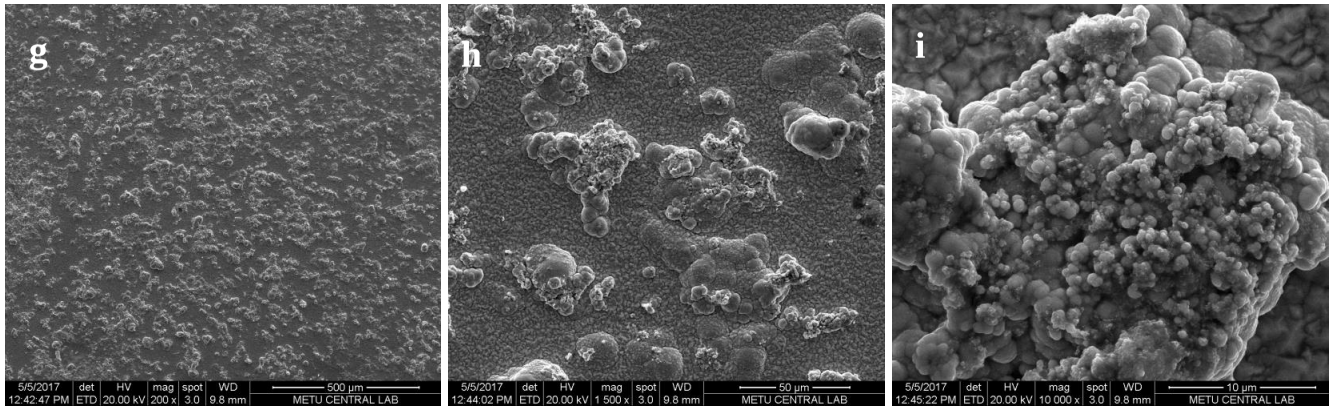

Figure 4.14 SEM micrographs for Ni/TiC nanocomposite produced in a Watts bath containing 5 g L^{-1} TiC and 125 ppm PEI at a magnification of (g) x200, (h) x1500 and (i) x10000. Current density and rotation speed are -50mA cm^{-2} and 100 rpm for all experiments, respectively.

Figure 4.13a-c shows that pure nickel has relatively smooth surface with pyramidal structure. This structure was already reported in the literature [21, 22, 27, 28] and shown in Figure 2.1 [21]. It can be seen from Figure 4.13d-f that nanocomposites produced in Watts bath without PEI addition results in non-uniform distribution of TiC with cauliflower structure, which is consistent with the literature [21, 22]. Moreover, the addition of PEI enhances the distribution of TiC and also TiC incorporation into the growing nickel film (Figure 4.14g-i). When Figure 4.13a and Figure 4.14g are compared, it is clearly seen that surface roughness of the nanocomposite is greater than pure nickel coating due to globular growth of Ni/TiC composite. Moreover, much smaller size of the globes is observed at a magnification of x10000 for nanocomposites produced in the presence of PEI (Figure 4.14i) than for nanocomposites produced in the absence of PEI (Figure 4.13f). Thus, PEI provides effective dispersion of TiC nanoparticles in the deposit and prevents agglomeration. According to Figure 4.14g-i, crack-free nanocomposites are achieved. Therefore, it can be said that hydrogen embrittlement due to hydrogen evolution is not a problem for a PEI electrolyte concentration of 125 ppm. The surface morphology of Ni/TiC nanocomposite is quite different than nickel coating as expected [21, 22].

In order to investigate the uniformity of TiC distribution in the deposit further, Ti mapping is performed. Figure 4.15 presents the Ti map for the Ni/TiC nanocomposite produced in a Watts bath containing 5 g L^{-1} TiC and 125 ppm PEI at current density of -50 mA cm^{-2} and rotation speed of 100 rpm.

According to Figure 4.15, few agglomerates of TiC in the deposit are detected. However, it can be concluded that the deposit shows uniformly distributed TiC nanoparticles with the addition of 125 ppm PEI into the electrolyte.

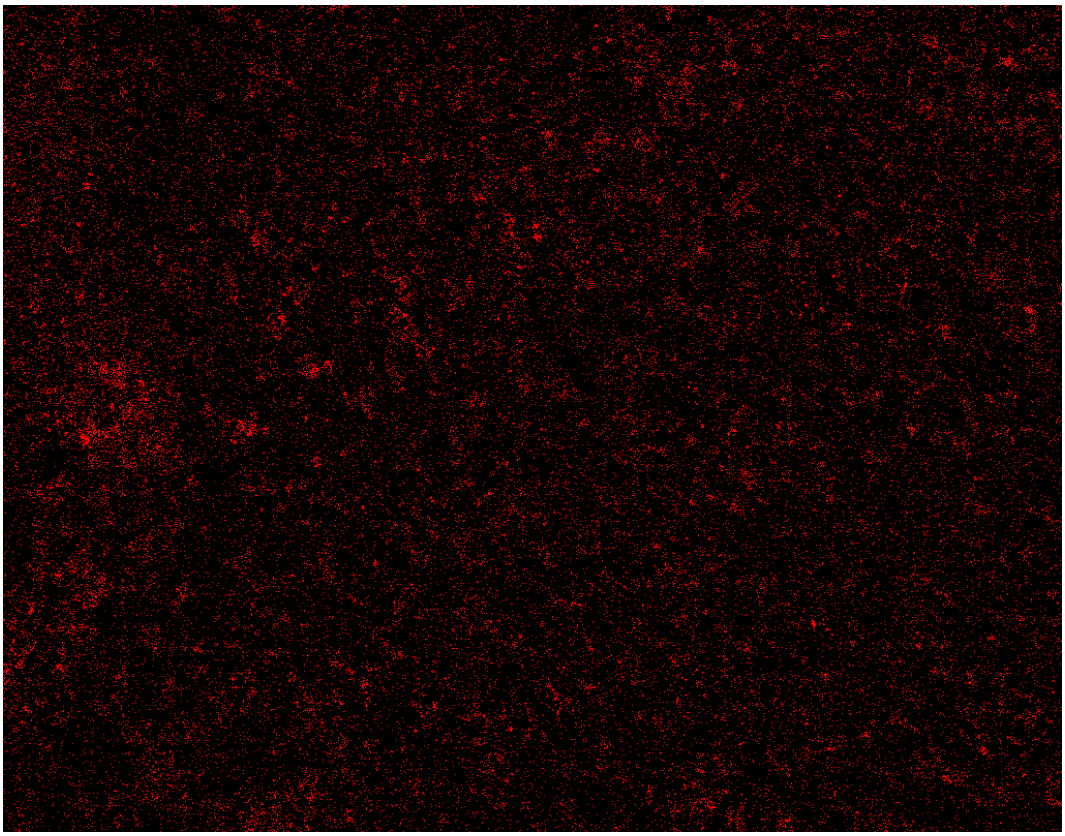

Figure 4.15 Ti map for the Ni/TiC nanocomposite at a magnification of x1000 (3.01 vol.% TiC in the deposit)

4.5. Characterization of Mechanical Properties of Nanocomposites

In order to characterize the mechanical properties, nanoindentation hardness of pure Ni coating and selected Ni/TiC nanocomposites are measured. Thickness of the coating is approximately 20 μm for all samples. All measurements are conducted at least 6 times on the same sample to calculate an average hardness value. Figure 4.16 shows a typical indentation plot for the Ni/TiC nanocomposites. By taking the arithmetical average of these measurements, nanoindentation hardness and Vicker's hardness are calculated and shown in Table 4.1.

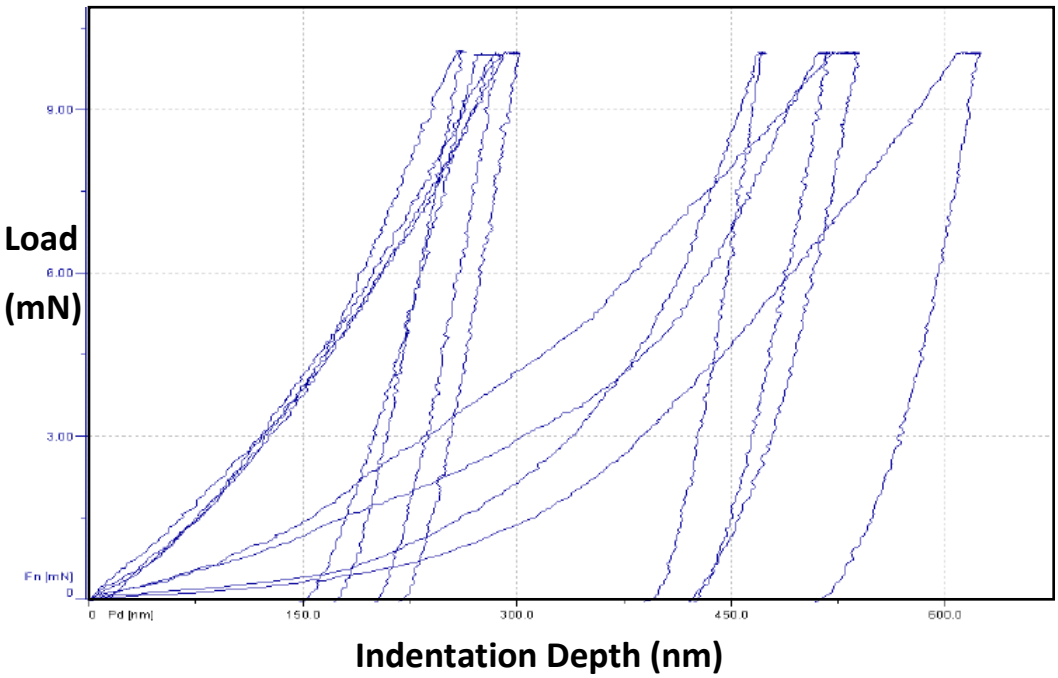

Figure 4.16 Typical indentation result for Ni/TiC nanocomposite produced in a Watts bath containing 5 g L^{-1} and 125 ppm PEI. The current density and rotation speed are -50 mA cm^{-2} and 100 rpm.

According to Figure 4.16, two types of characteristic behavior are observed for the two constituents of the nanocomposites, which are Ni and TiC. The harder material TiC results in less indentation depth under the same load compared to the Ni matrix.

Table 4.1 Hardness of pure nickel coating and Ni/TiC nanocomposites

Material/Property	**H_{IT} (GPa)**	**H (HV)**	**E (GPa)**
Pure Ni	2.07 ± 0.30	192 ± 24	107 ± 14
5 g L^{-1} TiC 125 ppm PEI -50 mA cm^{-2} 100 rpm (2.9 TiC vol.% in the deposit)	3.68 ± 2.55	352 ± 242	104 ± 51
5 g L^{-1} TiC 125 ppm PEI -25 mA cm^{-2} 900 rpm (5.4 TiC vol.% in the deposit)	2.19 ± 1.63	233 ± 166	72 ± 33

According to Table 4.1, pure nickel coating has lower hardness compared to the Ni/TiC nanocomposites as expected since TiC is already used as reinforcement to improve the mechanical properties of the metal matrix. The increase of hardness of Ni/TiC nanocomposites can be explained with two mechanisms; grain refining and dispersive strengthening [1]. Since incorporation and uniform distribution of TiC nanoparticles in the deposit suppresses the growth of Ni, smaller grain size of Ni matrix is achieved [1]. Smaller grain size leads to better mechanical properties. In addition, plastic deformation of the matrix is decreased by the dispersion of a harder phase [1]. However, when the Ni/TiC deposits are compared to each other, it is seen that the nanocomposite containing 2.9 vol.% TiC in the deposit produced by a current density of -50 mA cm^{-2} and rotation speed of 100 rpm has higher hardness than the nanocomposite containing 5.4 vol.% TiC in the deposit produced by a current density of -25 mA cm^{-2} and rotation speed of 900 rpm. In the literature, it was stated that the hardness of the Ni/TiC nanocomposite is directly proportional to the TiC amount in the deposit [1]. The probable reason that hardness of nanocomposite which has 5.4 vol.% TiC in the deposit is lower might be the non-uniformities of the sample produced at current density of -25 mA cm^{-2}. It was presented in Figure 4.10 that nanocomposites produced with a current density of -25 mA cm^{-2} had large standard deviation which may correspond to non-uniform TiC distribution. Therefore, the nanocomposite produced in a Watts bath containing 5 g L^{-1} TiC and 125 ppm PEI with a current density of -25 mA cm^{-2} and rotation speed of 900 rpm probably has non-uniform TiC amount and distribution which resulted in lower hardness than the nanocomposite produced in a Watts bath containing 5 g L^{-1} TiC and 125 ppm PEI with a current density of -50 mA cm^{-2} and rotation speed of 100 rpm. Yet, both nanocomposites have higher hardness than the pure nickel coating due to both grain refining and dispersive strengthening mechanisms.

According to the hardness measurements for Ni/TiC nanocomposites have larger standard deviations than the hardness measurements for pure nickel coating. Since

the indenter used for the analysis has a nanosized tip, hardness of two constituents of the nanocomposite which are Ni and TiC are measured separately. Therefore, taking the arithmetical average of the hardness values of two constituents resulted in such a large standard deviation. According to Table 4.1, average Vicker's hardness of pure nickel and two different Ni/TiC nanocomposites are reported as 192 HV, 352 HV and 233 HV. These values are comparable to the ones reported by Singh and Singh [18], who reported Vicker's hardness of nickel coating and Ni/TiC composite as 150 HV and 220 HV, respectively. It can be concluded that using TiC nanoparticles as a reinforcement increases the hardness of the composite. Moreover, elastic modulus of nickel coatings and Ni/TiC nanocomposites are similar to each other.

CHAPTER 5

CONCLUSIONS

The scope this work was the characterization of Ni/TiC electrodeposition in the presence of PEI in terms of the particle dispersion, electrodeposition kinetics, TiC amount in the deposit and morphological and mechanical properties of the composites. The critical parameters, which affect the co-deposition of Ni/TiC were ceramic particle properties, operating conditions and electrolyte composition.

The main novelty of this work is that it focuses on the investigation of the effect of the dispersant concentration on Ni/TiC electrodeposition in terms of the particle dispersion, electrodeposition kinetics, TiC amount in the deposit and morphological and mechanical properties of the composites. Watts solution containing TiC nanoparticles and PEI was preferred as the electrolyte. Three electrode system was set up by immersing the CE (nickel), RE and RDE in the electrolyte. The electrodeposition was performed under DC. Moreover, zeta potential measurements for the characterization of TiC particle stability in the electrolyte, LSV and current efficiency measurements for the characterization of electrodeposition kinetics, SEM/EDS for the characterization of TiC amount in the deposit and SEM, Ti mapping and hardness measurements for the morphological and mechanical characterization of Ni/TiC nanocomposites were utilized.

According to the zeta potential measurements, it can be concluded that even low concentrations, PEI addition resulted in a significant improvement of the dispersion of TiC nanoparticles in the electrolyte.

Polarization curves for different PEI electrolyte concentrations show that while the addition of PEI up to 125 ppm did not inhibit the electrodeposition remarkably except at low current densities, PEI addition of 250 ppm suppressed nickel electrodeposition significantly due to the adsorption of the polymer on the cathode. Moreover, current efficiency measurements indicate that the addition of PEI up to 125 ppm PEI resulted in an insignificant decrease of the current density from 97 % to 96.2%. Yet, increasing PEI electrolyte concentration up to 250 ppm decreased the current efficiency to 58.5 %, which is consistent with the significant shift of the polarization curve corresponding to 250 ppm PEI electrolyte concentration.

The effect of PEI on the TiC incorporation into the deposit was studied for different TiC electrolyte concentrations. One of the most important result of this work is that 125 ppm PEI addition to a Watts solution containing 5 g L^{-1} TiC enhanced particle dispersion effectively and increased TiC vol.% in the deposit from 0.68 % to 3.01 % without inhibiting nickel electrodeposition (current efficiency of 96.2%). Further increase of PEI electrolyte concentration up to 200 ppm caused a sharp decrease on the TiC incorporation. For the nanocomposites produced in a Watts bath containing 10 g L^{-1} TiC, a similar trend was observed. However, for the case of nanocomposites produced in a Watts bath containing 20 g L^{-1} TiC, increasing the PEI concentration resulted in a slight increase on the TiC incorporation since the addition of PEI at this concentration might not be sufficient to accomplish well dispersion of the particles in the electrolyte. The effect of TiC electrolyte concentration on TiC incorporation was also presented. It was concluded that increasing TiC electrolyte concentration from 5 g L^{-1} to 20 g L^{-1} did not change TiC vol.% in the deposit significantly. In addition, the effect of current density on TiC amount in the deposit was investigated; TiC incorporation

remained nearly unchanged with respect to current density in the absence of PEI. However, in the case of 125 ppm PEI addition, increasing current density resulted in decreasing TiC vol.% in the deposit due to the domination of nickel deposition over the incorporation of TiC. Finally, it was observed that TiC amount in the deposit increased with increasing rotation speed for PEI concentrations in the absence of PEI. On the other hand, TiC amount in the deposit was a weak function of rotation speed in the presence of 125 ppm PEI.

Morphological characterization of the nanocomposites showed that the addition of PEI up to 150 ppm decreased the agglomeration of TiC and provided uniformly distributed TiC in the deposit. However, further increase in the PEI concentration resulted in non-uniformities in the nanocomposite. For nanocomposites deposited in the absence of PEI, increasing rotation speed led to more uniform distribution of TiC in the deposit with less agglomeration. Yet, in the presence of 125 ppm PEI in the electrolyte, the effect of rotation speed on the morphology was insignificant. When Ni/TiC nanocomposites were compared with a pure nickel coating, cauliflower structure versus pyramidal structure were observed, respectively. Furthermore, PEI prevented the agglomeration of TiC nanoparticles since smaller globe-like TiC particles were observed in the presence of PEI. Finally, Ti mapping results also confirmed the uniformity of the nanocomposites. Moreover, hardness of Ni/TiC nanocomposites was higher than pure nickel composites.

This work provides important knowledge on electrodeposition and characterization of Ni/TiC electrodeposition in the presence of PEI in order to obtain high particle amount in the deposit with good particle dispersion without affecting electrodeposition kinetics. Therefore, this work is critical for the production of Ni/TiC in industrial applications. For future studies, in addition to nanoindentation hardness test, performing other mechanical tests such as Vicker's test and tribological tests will be useful for the characterization of the Ni/TiC nanocomposites further. Finally, scale-up studies on electrodeposition of Ni/TiC nanocomposites is recommended for future work.

REFERENCES

[1] M. Karbasi, N. Yazdian, and A. Vahidian, "Development of electro-co-deposited Ni-TiC nano-particle reinforced nanocomposite coatings," *Surf. Coatings Technol.*, vol. 207, pp. 587–593, 2012.

[2] M. Raja, G. N. K. R. Bapu, J. Maharaja, and R. Sekar, "Electrodeposition and characterisation of Ni– TiC nanocomposite using Watts bath," *Surf. Eng.*, 2014.

[3] T. Fuchigami, M. Atobe, and S. Inagi, *Fundamentals and applications of organic electrochemistry: synthesis, materials, devices*. Chichester, West Sussex: John Wiley & Sons, Ltd., 2015.

[4] A. C. West, *Electrochemistry and Electrochemical Engineering, An Introduction*. CreateSpace Independent Publishing Platform, 2012.

[5] D. Eroglu, "Modeling and Characterization of Rate Phenomena in Complex Electrochemical Systems: Sodium-Metal Chloride Batteries and Ni/SiC Co-Deposition," Colombia University, 2013.

[6] D. Eroglu and A. C. West, “Mathematical Modeling of Ni/SiC Co-Deposition in the Presence of a Cationic Dispersant,” *J. Electrochem. Soc.*, vol. 160, no. 9, pp. D354–D360, 2013.

[7] N. Guglielmi, “Kinetics of the Deposition of Inert Particles from Electrolytic Baths,” *J. Electrochem. Soc.*, vol. 119, no. 8, p. 1009, 1972.

[8] S. C. Wang and W. C. J. Wei, “Kinetics of electroplating process of nano-sized ceramic particle/Ni composite,” *Mater. Chem. Phys.*, vol. 78, no. 3, pp. 574–580, 2003.

[9] J. P. Celis, J. R. Roos, and C. Buelens, “A Mathematical Model for the Electrolytic Codeposition of Particles with a Metallic Matrix,” *J. Electrochem. Soc.*, vol. 134, no. 6, pp. 1402–1408, 1987.

[10] J. Fransaer, J. P. Celis, and J. R. Roos, “Analysis of the Electrolytic Codeposition of Non-Brownian Particles with Metals,” *J. Electrochem. Soc.*, vol. 139, no. 2, p. 413, 1992.

[11] G. Maurin and A. Lavanant, “Electrodeposition of nickel/silicon carbide composite coatings on a rotating disc electrode,” *J. Appl. Electrochem.*, vol. 25, no. 12, pp. 1113–1121, 1995.

[12] B. J. Hwang and C. S. Hwang, “Mechanism of Codeposition of Silicon Carbide with Electrolytic Cobalt,” *J. Electrochem. Soc.*, vol. 140, no. 4, pp. 979–984, 1993.

[13] P. M. Vereecken, I. Shao, and P. C. Searson, “Particle Codeposition in Nanocomposite Films,” *J. Electrochem. Soc.*, vol. 147, no. 7, pp. 2572–2575, 2000.

[14] P. Bercot, E. Pena-Munoz, and J. Pagetti, “Electrolytic composite Ni-PTFE coatings: An adaptation of Guglielmi’s model for the phenomena of incorporation,” *Surf. Coatings Technol.*, vol. 157, no. 2–3, pp. 282–289, 2002.

[15] C. T. J. Low, R. G. A. Wills, and F. C. Walsh, “Electrodeposition of composite coatings containing nanoparticles in a metal deposit,” *Surf. Coat. Technol.*, vol. 201, pp. 371–383, 2006.

[16] G. E. Dieter, D. Bacon, S. M. Copley, C. a Wert, and G. L. Wilkes, *Mechanical Metallurgy*. 1988.

[17] A. Hovestad and L. J. J. Janssen, “Electrochemical codeposition of inert particles in a metallic matrix,” *J. Appl. Electrochem.*, vol. 25, pp. 519–527, 1995.

[18] D. K. Singh, M. K. Tripathi, and V. B. Singh, “Preparation of Ni-TiC Nanocomposites by Electrolytic Codeposition from a Non Aqueous Bath and Their Characterization,” *J. Electrochem. Soc.*, vol. 159, no. 8, pp. 469–472, 2012.

[19] D. K. Singh and V. B. Singh, “Electrodeposition and characterization of Ni-TiC composite using N-methylformamide bath,” *Mater. Sci. Eng. A*, vol. 532, pp. 493–499, 2012.

[20] A. Asadi, M. Zandrahimi, R. Ebrahimi-Kahrizsangi, A. Saidi, and S. M. Seyedalangi, “New procedure for electrochemical production of Ni–TiC composite powder,” *Powder Metall.*, vol. 53, no. 1, pp. 47–50, 2010.

[21] Z. Yang, H. Lu, Z. Liu, X. Yan, and D. Li, “Effect of particle size on the surface activity of TiC– Ni composite coating via the interfacial valence electron localization,” *RSC Adv.*, vol. 6, pp. 18793–18799, 2016.

[22] E. Dănăilă, L. Benea, N. Caron, and O. Raquet, “Titanium Carbide Nanoparticles Reinforcing Nickel Matrix for Improving Nanohardness and Fretting Wear Properties in Wet Conditions,” *Met. Mater. Int*, vol. 22, no. 5, pp. 924–934, 2016.

[23] L. Benea, N. Ege Caron, and O. Raquet, “Tribological behavior of a Ni matrix hybrid nanocomposite reinforced by titanium carbide nanoparticles during electro-codeposition,” *RCS Adv.*, vol. 6, pp. 59775–59776, 2016.

[24] C. M. P. Kumar and T. V. Venkatesha, “Characterization and Corrosion Behavior of Electrodeposited Zn and Zn-BN Coatings,” *Synth. React. Inorganic, Met. Nano-Metal Chem.*, vol. 42, no. 3, pp. 351–359, 2012.

[25] N. D. Lang and W. Kohn, “Theory of metal surfaces: Work function,” *Phys. Rev. B*, vol. 3, no. 4, pp. 1215–1223, 1971.

[26] W. Li and D. Y. Li, “Influence of surface morphology on corrosion and electronic behavior,” *Acta Mater.*, vol. 54, no. 2, pp. 445–452, 2006.

[27] S. Mosleh-Shirazi, G. Hua, F. Akhlaghi, X. Yan, and D. Li, “Interfacial valence electron localization and the corrosion resistance of Al-SiC nanocomposite,” Nature Publishing Group, 2015.

[28] S. Mohajeri, A. Dolati, and S. Rezagholibeiki, “Electrodeposition of Ni/WC nano composite in sulfate solution,” *Mater. Chem. Phys.*, vol. 129, no. 3, pp. 746–750, 2011.

[29] P. Gyftou, E. A. Pavlatou, and N. Spyrellis, “Effect of pulse electrodeposition parameters on the properties of Ni/nano-SiC composites,” *Appl. Surf. Sci.*, vol. 254, no. 18, pp. 5910–5916, 2008.

[30] A. C. Vieira, A. R. Ribeiro, L. A. Rocha, and J. P. Celis, “Influence of pH and corrosion inhibitors on the tribocorrosion of titanium in artificial saliva,” *Wear*, vol. 261, no. 9, pp. 994–1001, 2006.

[31] MP Biomedicals, "www.mpbio.comproduct.phppid=05218151&country=215.pdf." .

[32] J. Sun and L. Gao, "Dispersing SiC powder and improving its rheological behaviour," *J. Eur. Ceram. Soc.*, vol. 21, no. 13, pp. 2447–2451, 2001.

[33] J. X. Zhang, D. L. Jiang, S. H. Tan, L. H. Gui, and M. L. Ruan, "Aqueous processing of SiC green sheets I: Dispersant," *J. Mater. Res.*, vol. 17, no. 8, pp. 2012–2018, 2002.

[34] Y. Zhang and J. Binner, "Effect of dispersants on the rheology of aqueous silicon carbide suspensions," *Ceram. Int.*, vol. 34, pp. 1381–1386, 2008.

[35] J. Zhang, L. Duan, D. Jiang, Q. Lin, and M. Iwasa, "Dispersion of TiN in aqueous media," *J. Colloid Interface Sci.*, vol. 286, pp. 209–215, 2005.

[36] E. Laarz and L. Bergström, "Dispersing WC-Co powders in aqueous media with polyethylenimine," *Int. J. Refract. Met. Hard Mater.*, vol. 18, pp. 281–286, 2000.

[37] H. Foratirad, H. R. Baharvandi, and M. G. Maragheh, "Effects of dispersants on dispersibility of titanium carbide aqueous suspension," *Int. J. Refract. Met. Hard Mater.*, vol. 56, pp. 96–103, 2016.

[38] S.-K. Kim, D. Josell, and T. P. Moffat, “Electrodeposition of Cu in the PEI-PEG-Cl-SPS Additive System Reduction of Overfill Bump Formation During Superfilling,” *J. Electrochem. Soc.*, vol. 153, no. 9, pp. C616–C622, 2006.

[39] S.-K. Kim, J. E. Bonevich, D. Josell, and T. P. Moffat, “Electrodeposition of Ni in Submicrometer Trenches,” *J. Electrochem. Soc.*, vol. 154, no. 9, pp. D443–D451, 2007.

[40] D. Eroglu, A. Vilinska, P. Somasundaran, and A. C. West, “Effect of a Cationic Polymer, Polyethyleneimine, on Ni/SiC Co-Deposition,” *J. Electrochem. Soc.*, vol. 160, no. 2, pp. D35-40, 2013.

[41] D. Eroglu, A. Vilinska, P. Somasundaran, and A. C. West, “Use of dispersants to enhance incorporation rate of nano-particles into electrodeposited films,” *Electrochim. Acta*, vol. 113, pp. 628–634, 2013.

[42] A. Vilinska *et al.*, “Stabilization of Silicon Carbide (SiC) micro- and nanoparticle dispersions in the presence of concentrated electrolyte,” *J. Colloid Interface Sci.*, vol. 423, pp. 48–53, 2014.

[43] F. C. Walsh and C. Ponce de Leon, “A review of the electrodeposition of metal matrix composite coatings by inclusion of particles in a metal layer: an established and diversifying technology,” *Trans. IMF*, vol. 92, no. 2, pp. 83–98, 2014.

[44] F. C. Walsh, C. T. J. Low, and J. O. Bello, “Influence of surfactants on electrodeposition of a Ni-nanoparticulate SiC composite coating,” *Trans. IMF*, vol. 93, no. 3, pp. 147–156, 2015.

[45] A. Fahami, B. Nasiri-Tabrizi, M. Rostami, and R. Ebrahimi-Kahrizsangi, “Influence of surfactants on the characteristics of Nickel matrix nanocomposite coatings,” *ISRN Electrochem.*, vol. 2013, pp. 1–8, 2013.

[46] H. Foratirad, H. R. Baharvandi, and M. G. Maragheh, “Chemo-Rheological Behavior of Aqueous Titanium Carbide Suspension and Evaluation of the Gelcasted Green Body Properties,” *Mater. Res.*, vol. 20, no. 1, pp. 175–182, 2017.

[47] Nanografi Nano Technology, “Titanium Carbide (TiC , 99 + %, 40-60nm , cubic).”

[48] Sigma-Aldrich, “Polyethylene Imine Product Specification.”

[49] J. Newman and K. E. Thomas-Alyea, *Electrochemical Systems*. 2004.

[50] N. Mep and J. Newman, “This Week ’ s Citation Classic,” p. 1983, 1983.

[51] Pine Research Instrumentation, “Rotating Disk Electrode Product Guide,” 2016.

[52] Pine Research Instrumentation, “Reference Electrode Product Guide,” 2017.

[53] nanoComposix, “Schematic of the electrical double later at the surface of solution-phase nanoparticles.” [Online]. Available: https://nanocomposix.com/pages/characterization-techniques.

[54] “Zeta Potential An Introduction in 30 Minutes.” [Online]. Available: file:///C:/Users/User/Downloads/mrk654-01_an_introduction_to_zeta_potential_v3.pdf. [Accessed: 01-Jan-2017].

[55] R. G. Ehl and A. J. Ihde, “Faraday’s electrochemical laws and the determination of equivalent weights,” *J. Chem. Educ.*, vol. 31, no. 5, pp. 226–232, 1954.

[56] Anderson Materials Evaluation, “SEM Illustrative Example : Secondary Electron and Backscatter Electron Images.” [Online]. Available: http://www.andersonmaterials.com/sem/sem-secondary-backscatter-images.html.

[57] W. C. Oliver and G. M. Pharr, “Measurement of hardness and elastic modulus by instrumented indentation: Advances in understanding and refinements to methodology,” *J. Mater. Res.*, vol. 19, no. 1, pp. 3–20, 2004.

APPENDIX A

SAMPLE CALCULATIONS

FOR THE TITANIUM CARBIDE VOL.% IN THE NANOCOMPOSITE

Calculation of TiC vol.% in the deposit

- Ti wt.% of nanocomposites are measured for 5 different points on the three parallel nanocomposites by using EDS. Figure A.1 represents locations of these measurements.

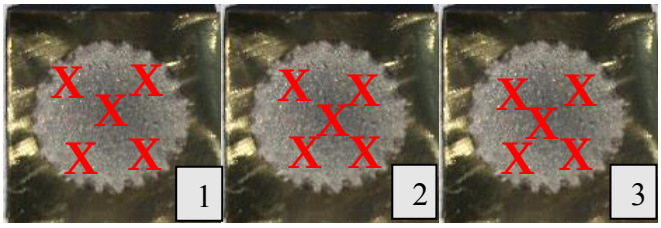

Figure A.1 Locations of EDS measurements for three samples

- For instance, for nanocomposite produced in Watts bath containing 5 g L^{-1} TiC and 125 ppm PEI at a current density of -50 mA cm^{-2} and rotation speed of 100 rpm EDS results in terms of Ti wt.% are shown in Table A.1.

Table A.1 EDS results in terms of Ti wt.%

Sample no/ location	Center	Top-right	Top-left	Bottom-left	Bottom-right
1	0.672	1.058	0.831	1.006	1.142
2	1.619	1.471	0.878	1.317	1.358
3	2.003	1.550	1.832	2.327	1.257

- Ti wt.% is converted to TiC vol.% in the deposit by using Equation 3.5.

$$TiC\ vol.\% = \frac{Ti\ wt.\% \times \frac{M_{TiC}}{M_{Ti}} \times \frac{1}{\rho_{TiC}}}{Ti\ wt.\% \times \frac{M_{TiC}}{M_{Ti}} \times \frac{1}{\rho_{TiC}} + Ni\ wt.\% \times \frac{1}{\rho_{Ni}}}$$

where;

$M_{TiC} = 59.89\ g\ mol^{-1}$

$M_{Ti} = 47.867\ g\ mol^{-1}$

$\rho_{TiC} = 4.93\ g\ cm^{-3}$

$\rho_{Ni} = 8.908\ g\ cm^{-3}$

For 1st sample, measurement at the center which corresponds 0.672 wt.% Ti, TiC vol.% is calculated as;

$$TiC\ vol.\% = \frac{0.672 \times \frac{59.89}{47.867} \times \frac{1}{4.93}}{0.672 \times \frac{59.89}{47.867} \times \frac{1}{4.93} + 99.328 \times \frac{1}{8.908}} = 1.506$$

For 2nd sample, measurement at the center which corresponds 1.619 wt.% Ti, TiC vol.% is calculated as;

$$TiC\ vol.\% = \frac{1.619 \times \frac{59.89}{47.867} \times \frac{1}{4.93}}{1.619 \times \frac{59.89}{47.867} \times \frac{1}{4.93} + 98.381 \times \frac{1}{8.908}} = 3.587$$

Therefore, Table A.1 can be rewritten in terms of TiC vol.% and shown in Table A.2 by taking arithmetical average of 5 measurements from different locations.

Table A.2 EDS results in terms of TiC vol.%

Sample no/ location	Center	Top-right	Top-left	Bottom-left	Bottom-right	Average
1	1.506	2.36	1.859	2.246	2.545	2.103
2	3.587	3.265	1.963	2.929	3.018	2.952
3	4.417	3.437	4.048	5.111	2.797	3.962

Finally, arithmetical average and standard deviation of three samples are calculated and presented below.

$$TiC\ vol.\%\ average = \frac{2.103 + 2.952 + 3.962}{3} = 3.01$$

$$standard\ deviation$$

$$= \sqrt{\frac{(2.103 - 3.01)^2 + (2.952 - 3.01)^2 + (3.962 - 3.01)^2}{3}} = 0.76$$

Therefore, TiC vol.% in the deposit is represented as 3.01 ± 0.76%.